Beyond the CpG: an integrative approach to decoding DNA methylation in immunometabolic health

Sinke, L.J.

CHAPTER SIX

Growing Old TOgether

Tissue-specific methylomic responses to a lifestyle intervention in older adults associate with metabolic and physiological health improvements

Lucy Sinke[1], Marian Beekman[1], Yotam Raz[1], Thies Gehrmann[1,2], Ioannis Moustakas[1], Alexis Boulinguiez[3], Nico Lakenberg[1], Eka Suchiman[1], Fatih A. Bogaards[1,4], Daniele Bizzarri[1,5], Erik B. van den Akker[1,5], Melanie Waldenberger[6,7], Gillian Butler-Browne[3], Capucine Trollet[3], C. P. G. M. Lisette de Groot[4], Bastiaan T. Heijmans[1], and P. Eline Slagboom[1]

[1] Leiden University Medical Centre, Leiden, The Netherlands
[2] University of Antwerp, Antwerp, Belgium
[3] Sorbonne University, Paris, France
[4] Wageningen University and Research, Wageningen, The Netherlands
[5] Delft Bioinformatics Lab, Delft, The Netherlands
[6] Helmholtz Munich, Neuherberg, Germany
[7] German Centre for Cardiovascular Research (DZHK), Munich, Germany

Published in Aging Cell 24(4):e14431 (2025)
DOI: 10.1111/acel.14431

Abstract

Across the lifespan, diet and physical activity profiles substantially influence immunometabolic health. DNA methylation, a tissue-specific epigenetic marker sensitive to behavioural change, may mediate these effects through modulation of transcription factor binding and subsequent gene expression. Despite this, few human studies have profiled DNA methylation and gene expression simultaneously in multiple tissues or examined how molecular levels react and interact in response to lifestyle changes.

The Growing Old Together (GOTO) study was a 13-week lifestyle intervention in older adults, which imparted health benefits to participants. Here, we characterised the DNA methylation response to this intervention at over 750,000 CpGs in muscle, adipose, and blood. Differentially methylated sites were enriched for active chromatin states, located close to relevant transcription factor binding sites, and associated with alterations in insulin sensitivity genes and health parameters. In addition, measures of biological age were consistently reduced by the intervention and decreases in grimAge could be connected to observed health improvements. Taken together, our results reveal and interrogate sets of responsive tissue-specific loci and outline their potential to measure progression and finetune treatment of age-related risks and diseases.

Graphical Abstract

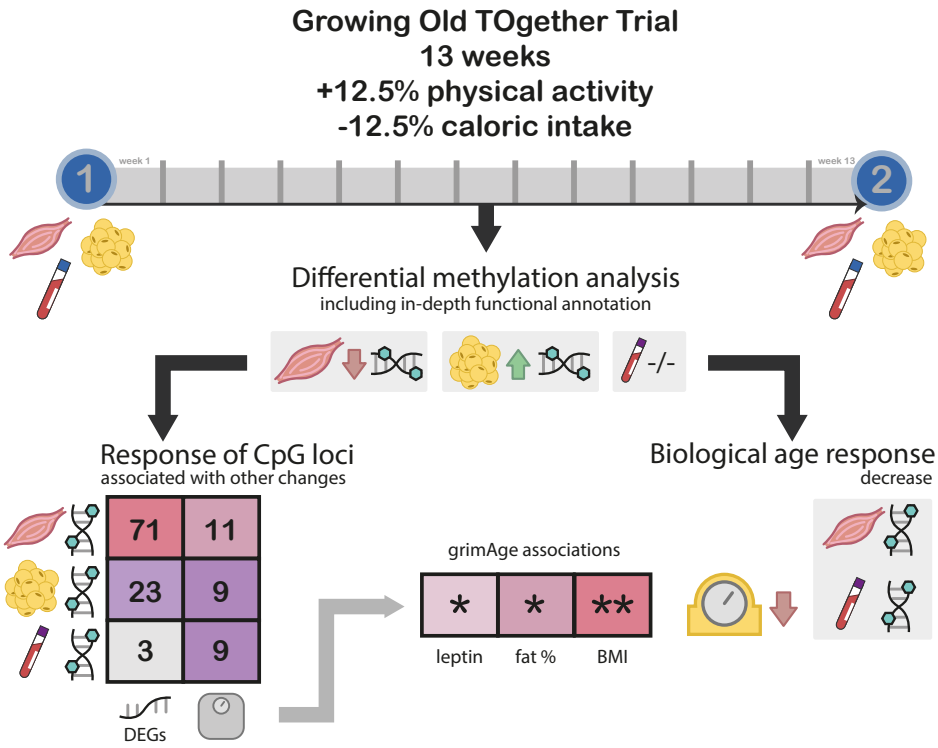

Highlights

- DNA methylation and gene expression are profiled in three tissues before and after a 13-week lifestyle intervention in older adults.
- Differentially methylated sites predominantly reside in active chromatin in close proximity of transcription factor binding sites.
- This methylation response correlates with differential expression of insulin sensitivity genes in muscle and adipose tissues.
- Changes in all three tissues associate with decreases in body fat percentage and leptin levels.
- Tissue-specific epigenetic age algorithms can capture intervention effects and connect them to observed health improvements.

Keywords: *DNA methylation, epigenomics, functional genomics, healthy ageing, lifestyle, metabolism, muscle*

Background

Changes in behaviour across the life course, including adherence to healthy diets and physical activity regimens, have major health impacts. In some cases, they are more effective at improving immunometabolic health than pharmacological interventions[1–3]. Regular aerobic exercise alongside caloric restriction can promote weight loss, insulin sensitivity, and glucose control in both younger and older populations[4–7]. Epigenetic regulation, such as through DNA methylation (DNAm), may mediate a portion of these health benefits by modulating the accessibility of regulatory sites for transcription[8–10]. Physical activity has been found to attenuate the age-dependent decreases in DNAm of the anti-inflammatory *ASC* gene in blood[11,12], and Mendelian randomization has directionally linked epigenetic signatures of a healthy diet with both type 2 diabetes and several of its risk factors[13]. These findings highlight potential for DNAm in measurement and modification of immunometabolic health in individuals of all ages.

Whilst epigenomic responses to intervention studies have revealed promising results in blood, epigenetic reprogramming of other metabolic tissues may have even greater functional consequences on health[14]. Muscle and adipose tissues secrete a plethora of proteins and signalling molecules into the circulation and engage in tissue-to-tissue crosstalk, collectively bringing about clinically meaningful biological changes[15]. Although several experimental studies have investigated the effects of lifestyle interventions on the methylome of muscle[16,17] or adipose[18–20] individually, few researchers have taken a multi-tissue approach despite this showing promise in other-omic fields[21–23]. To advance our understanding of how epigenetics influences immunometabolic health, we must diversify and expand our study designs by incorporating relevant tissues, improving CpG coverage, and including the older adults who represent a growing proportion of our populations.

The Growing Old Together (GOTO) study is a 13-week lifestyle intervention in 164 older adults (mean age 63 years), which expanded on the combined intervention arm of the CALERIE study[24]. Here, we followed up on previous work indicating that the GOTO intervention conferred an immunometabolic health improvement to participants[25,26] and that this benefit associates with changes in the blood[27], adipose, and muscle transcriptomes[28] and the blood metabolome[29]. Using data and biomaterial from before and after the GOTO study, we profiled DNAm at over 750,000 CpG sites across the genome in skeletal muscle (n = 80), subcutaneous adipose (SAT, n = 89), and fasted blood tissues (n = 98). By thoroughly characterising the resulting loci, we examined how methylomic responses to the GOTO intervention relate to genomic regulation and differential gene expression in *cis*, with implications for immunometabolic health and epigenetic measures of chronological and biological age.

Results

The GOTO intervention improves metabolic health comparably across tissue-specific subsets of participants

The GOTO intervention (n = 164) imparted a range of metabolic health benefits, described in detail previously[25,27–29]. Notably, participants saw reductions in their body mass index (BMI, Δ = −1.1 kg/m^2), waist circumference (WC, Δ = −4.3 cm), and total body fat percentage (Δ = −1.8%) alongside improvements in other health measurements (**Table 1**). Baseline characteristics are shown in **Supplementary Table 1**. Individuals were selected for DNAm profiling based on availability of biological material and gene expression data, and for a majority (n = 66, 64.7%), data was collected from all three tissues both before and after the intervention.

	Entire GOTO population (n = 164)		Three tissue overlap (n = 66)		Skeletal muscle (n = 80)		Adipose tissue (n = 89)		Fasted blood (n = 98)	
	Δ(SE)	**Padj**	**Δ(SE)**	**Padj**	**Δ(SE)**	**Padj**	**Δ(SE)**	**Padj**	**Δ(SE)**	**Padj**
Body mass index (kg/m^2)	-1.13 (0.06)	2.0E-39	-1.24 (0.10)	1.2E-17	-1.28 (0.09)	4.2E-23	-1.27 (0.08)	1.5E-26	-1.28 (0.08)	1.9E-29
WC (cm)	-4.32 (0.42)	5.6E-19	-4.83 (0.66)	2.7E-09	-5.10 (0.60)	5.2E-12	-4.53 (0.58)	5.6E-11	-4.65 (0.55)	9.8E-13
Total body fat (%)	-1.76 (0.23)	8.7E-12	-2.13 (0.35)	2.3E-07	-2.03 (0.34)	9.4E-08	-2.18 (0.30)	2.7E-10	-2.05 (0.30)	1.9E-09
Fasting insulin (mU/L)	-0.31 (0.25)	2.7E-01	-0.83 (0.41)	5.8E-02	-0.55 (0.38)	1.7E-01	-0.45 (0.38)	2.7E-01	-0.46 (0.34)	2.0E-01
Systolic BP (mm Hg)	-3.15 (0.94)	1.6E-03	-2.82 (1.68)	1.1E-01	-2.66 (1.46)	1.0E-01	-2.88 (1.34)	4.9E-02	-2.51 (1.25)	6.8E-02
Leptin (µg/L)	-2.32 (0.34)	3.7E-10	-2.75 (0.44)	1.4E-07	-2.72 (0.38)	9.4E-10	-2.95 (0.40)	2.7E-10	-2.86 (0.37)	1.9E-11
Adiponectin (mg/L)	0.26 (0.14)	1.1E-01	0.52 (0.25)	5.8E-02	0.45 (0.21)	6.1E-02	0.27 (0.21)	2.5E-01	0.28 (0.20)	2.0E-01
Interleukin-6 (ng/L)	0.09 (0.11)	4.8E-01	0.30 (0.15)	5.8E-02	0.23 (0.31)	1.1E-01	0.24 (0.11)	4.9E-02	0.26 (0.12)	5.8E-02
HDL cholesterol (mmol/L)	-0.01 (0.02)	6.2E-01	0.00 (0.03)	9.3E-01	0.00 (0.03)	9.4E-01	-0.02 (0.02)	5.3E-01	-0.02 (0.02)	4.8E-01
Fasting HDL size (nm)	0.04 (0.01)	5.7E-09	0.06 (0.01)	1.3E-05	0.07 (0.01)	1.9E-08	0.05 (0.01)	6.6E-07	0.05 (0.01)	3.0E-08

Table 1 | Effects of the 13-week GOTO intervention on ten immunometabolic health measurements in the entire population and each tissue dependent subset. Associations were calculated using linear mixed models with fixed effects for age and sex and a random effect for ID.

Tissue-specific methylation subsets (muscle n = 80, SAT n = 89, and blood n = 98) were representative of the whole study population, with the distribution of changes in ten health parameters from included and excluded individuals being statistically comparable (nonresponse analysis $p_{FDR} \geq 0.05$; **Supplementary Table 2**). The sole exception was a selection bias for individuals with higher high-density lipoprotein (HDL) cholesterol sizes in the muscle subset ($p_{FDR} = 0.001$) urging caution in making inferences

about this trait in muscle analyses. In each tissue, we analysed the genome-wide DNAm consequences of the GOTO intervention, adjusting for age, sex, smoking status, technical covariates, and the first five principal components (PCs). In skeletal muscle and SAT samples, estimated bias and inflation of the test statistics was low ($|\mu| < 0.05$, $\lambda < 1.1$). In the blood samples, there was some deflation in the test statistics ($\lambda = 0.86$) alongside minimal bias ($\mu = 0.03$). For all tissues, bias and inflation of the test statistics was corrected for and residual values were under 0.01 and equal to 1.0 respectively, indicating high quality data.

In skeletal muscle, the GOTO intervention influenced DNAm at 162 predominantly hypomethylated CpGs

To interrogate the muscle methylomic response, we profiled DNAm in skeletal muscle samples biopsied before and after the GOTO intervention (n = 160 samples, 80 individuals). Since cell-type proportions can be an important driver of epigenetic signals, we predicted proportions of seven muscle nuclei types in our samples by applying the *MuSiC* deconvolution algorithm[30] to bulk gene expression data and a publicly available single nuclei reference transcriptome[31]. At baseline, our samples were primarily composed of slow (type I, mean 36.0%) and fast (type II, mean 26.7%) skeletal muscle fibres and endothelial cells (mean 36.6%). Following the intervention, the proportion of predicted endothelial nuclei had increased (Δ = +3.3%, p_{FDR} = 3.5E−03), in line with expected angiogenesis during the intervention[32]. There was insufficient evidence to suggest changes for any other nuclei type ($p_{FDR} \geq 0.05$; **Fig. 1a; Supplementary Table 3**).

In our initial unadjusted model, we identified 354 differentially methylated CpGs following the intervention ($p_{FDR} < 0.05$). However, considering the finding that an increase in endothelial nuclei could have been driving a portion of this methylation signal, we further adjusted our model for predicted endothelial nuclei proportions. This led to the removal of 192 CpGs from our results, leaving 162 predominantly hypomethylated (87.7%) CpGs where DNAm changes were independent of endothelial nuclei proportions ($p_{fdr} < 0.05$; **Fig. 1b; Supplementary Table 4**). Henceforth, we refer to this set of 162 differentially methylated CpGs in skeletal muscle, which represented 160 distinct loci, as the *muscle CpGs*.

CpGs influenced by the GOTO intervention associate with genes important for translocation of GLUT4 to the muscle cell membrane

To investigate potential for the *muscle CpGs* to regulate nearby gene expression, we annotated their genomic positions to 15 chromatin states using reference epigenomes from the Roadmap Epigenomics Consortium[33]. These consisted of eight active and seven repressed configurations that show distinct levels of DNAm, accessibility, and regulator binding. By testing if the *muscle CpGs* were enriched for specific genomic features in the

male (E107) and female (E108) skeletal muscle reference, we revealed that both enhancers (OR_{E107} = 5.83; OR_{E108} = 7.15) and genic enhancers (OR_{E107} = 3.56; OR_{E108} = 4.34) were overrepresented in our results (**Fig. 1c; Supplementary Table 5**). Since the primary mechanism that DNAm influences nearby expression is through transcription factor (TF) binding, we also tested if sequences within 50 bp of the *muscle CpGs* were enriched for known TF binding sites compared to a GC-matched random background (TFBS; **Fig. 1d; Supplementary Table 6**)[34]. The tested regions were enriched for 21 TFBS including ones upregulated by exercise (JunB: 34 CpGs)[35] and critical for muscle regeneration (Fos: 35 CpGs; Fra1: 33 CpGs)[36–38].

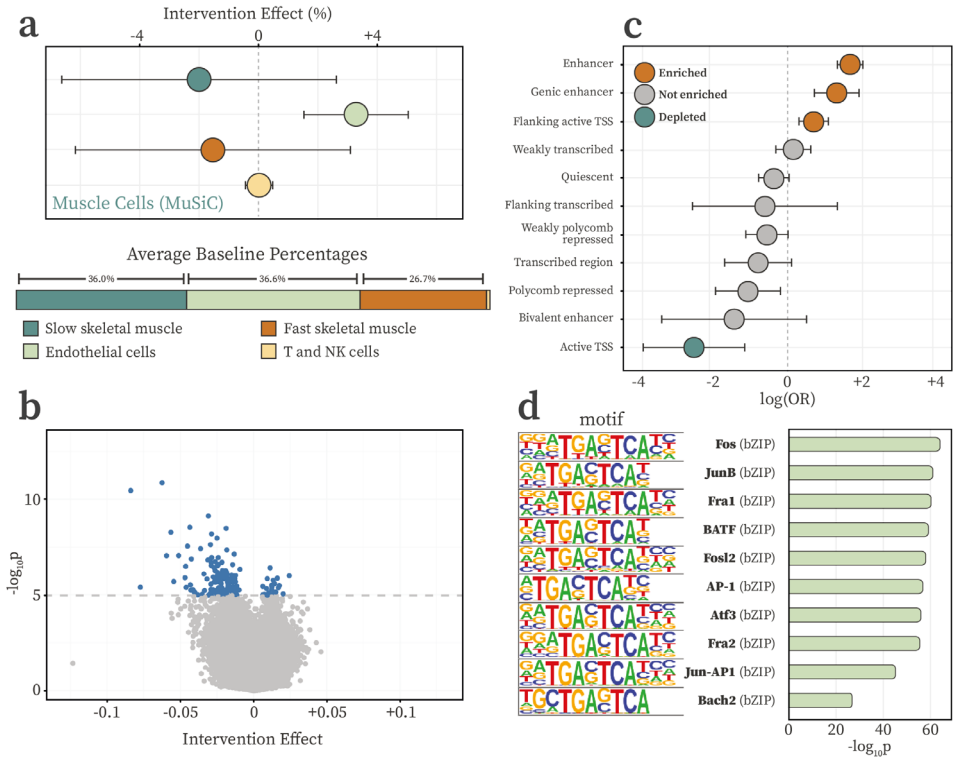

Figure 1 | Characterisation of the muscle cell count and DNAm response to the GOTO intervention. a) Intervention effect on predicted muscle nuclei types alongside baseline proportions (only cells >0.5% at baseline shown). **b)** Volcano plot of the intervention effect on DNAm in muscle at over 750,000 CpGs, showing 162 differentially methylated (blue) and non-significant CpGs (grey). **c)** Forest plot of the odds ratio (OR) and 95% confidence intervals (CIs) for enrichment (orange) or depletion (blue) of 11 chromatin states investigated using the male skeletal muscle reference epigenome from the Roadmap Epigenomics Consortium (E107; four states with extremely wide CIs not shown). **d)** Bar plot of the top ten transcription factor binding site (TFBS) motifs enriched in sequences within 50 bp of identified CpGs when compared to a GC-matched random genomic background.

Having established the *muscle CpGs* as plausibly regulatory, we used a two-step approach to identify their candidate target genes. First, we evaluated if expression of genes in close proximity (±100 kb) to the 162 muscle CpGs was altered by the intervention using available RNA-seq data ($p_{FDR} < 0.05$)[28]. Next, we examined whether these expression changes were associated with differential DNAm at the nearby CpG ($p_{FDR} < 0.05$). In total, there were 454 unique genes within 100kb of a muscle CpG, and 71 of these were both differentially expressed following the intervention and associated with the DNAm response in *cis* (**Supplementary Table 7**). This set of 71 genes included several directly implicated in the translocation of GLUT4 transporters to the muscle cell membrane in response to insulin and contractile activity (*TMOD3, FDFT1,* and *PLEKHG4*)[39–41] alongside an adaptor protein which regulates insulin signalling, specifically in skeletal muscle cells (*GRB10*)[42,43]. Over-representation analysis of these 71 genes revealed enrichment for *Striated Muscle Cell Development* after adjusting for multiple testing ($p_{FDR} = 0.019$), further clarifying the relevance of these genes to muscle-specific functions.

Altered blood-based health markers and grip strength associate with DNAm responses in skeletal muscle

We investigated whether the DNAm at the *muscle CpGs* was associated with changes in the ten immunometabolic health parameters shown in **Table 1** after adjusting for multiple testing (**Fig. 2a; Supplementary Table 8**). Methylation responses at 33 (20.4%) sites were connected to at least one blood-based trait, with eight CpGs linked to improvements in three or more traits ($p_{FDR} < 0.05$).

To explore if methylomic responses in muscle related to physiological adaptations within the same tissue, we expanded our analyses to include three additional muscle-specific phenotypes. This included average dominant hand grip strength as a marker of overall muscle performance, as well as two immunohistochemistry measures ($n = 65$, 81% of the original muscle subset; **Supplementary Table 9**)[44], namely the number of PAX7 positive cells and myonuclei per fibre. PAX7 is a satellite cell marker indicative of muscular regenerative potential[45], and higher numbers of myonuclei per fibre align with larger and stronger muscle fibres[46,47]. Both immunohistochemistry measures were associated with DNAm responses at more than 70 differentially methylated CpGs ($n_{MYO} = 75$, $n_{PAX7} = 84$), and DNAm at 36 CpGs was also correlated with average dominant hand grip strength. In total, over half of the *muscle CpGs* were linked to at least one of the investigated blood- or muscle-based traits, demonstrating relevance for this set of CpGs to observed health improvements ($n = 103$, 61.7%).

More specifically, there were 16 CpGs with multiple lines of evidence supporting their regulatory and clinical potential. These sites were differentially methylated, located in *cis* regulatory regions, and also associated with both differential gene expression and observed health benefits. An example of one such CpG was cg21005024, which was

hypomethylated following the GOTO intervention (β = −0.047) and flanks an active transcription start site (TSS) of *GRB10* within 50 bp of multiple enriched TFBS. DNAm at this CpG is also positively associated with *GRB10* expression (β = 0.083), WC (β = 0.003), and total body fat percentage (β = 0.005), and inversely correlated with both immunohistochemistry measures (β_{PAX7} = −0.220, β_{MYO} = −0.011) and average dominant hand grip strength (β = −0.004; **Fig. 2b**). Taken together, these findings highlighted *GRB10* as a responsive locus in muscle that may be under epigenetic control.

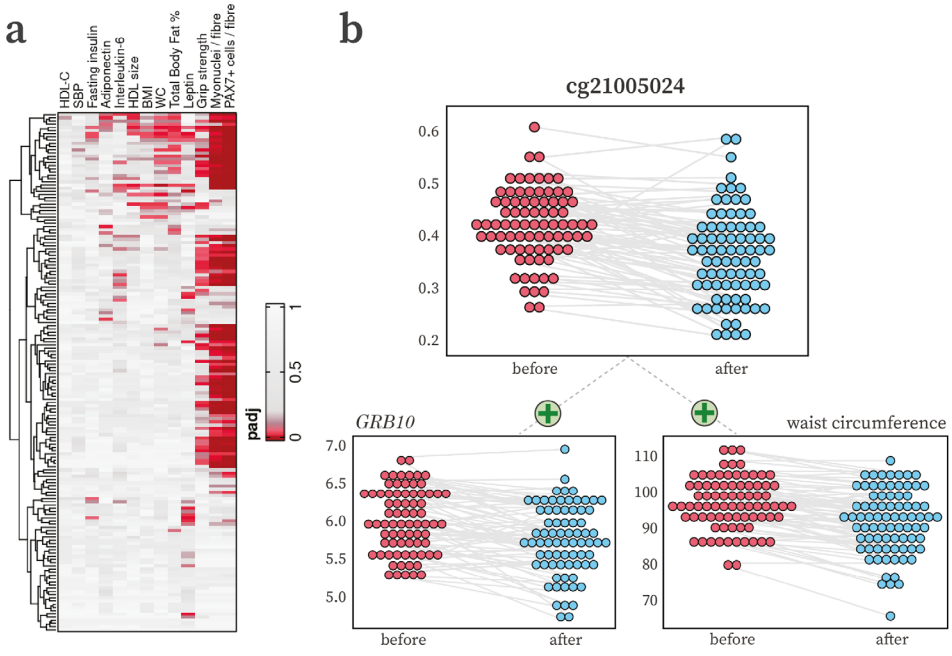

Figure 2 | Integrative analyses in muscle. a) Clustered heatmap of association *p*-values between changes in DNAm at the 162 *muscle CpGs* and thirteen health parameters (ten blood-based and three muscle-specific traits). **b)** Dot plots showing hypomethylation of DNAm in muscle at cg21005024, positively associated with both decreases in muscle *GRB10* gene expression and in waist circumference (HDL: high density lipoprotein; SBP: systolic blood pressure; BMI: body mass index; WC: waist circumference).

In adipose tissue, the GOTO intervention influenced DNAm at 230 predominantly hypermethylated CpGs

Next, we analysed DNAm responses in SAT following the GOTO intervention (n = 89 individuals, 178 samples). We identified 230 differentially methylated CpGs at 201 distinct loci ($p_{FDR} < 0.05$), henceforth referred to as the *adipose CpGs*. To explore whether this methylation signal was partially driven by changes in cell type proportions, we deconvoluted the bulk gene expression data using the *CIBERSORTx* algorithm[48] and a publicly available signature matrix[49] (**Fig. 3a; Supplementary Table 10**). The most prevalent cell types at baseline were adipocytes (mean 72.4%) followed by a large minority of microvascular endothelial cells (MVECs; mean 24.1%), and there was insufficient evidence to support a change in any of the predicted cell types following the intervention ($p_{FDR} \geq 0.05$). Therefore, further adjustment was not appropriate in these paired analyses as cellular composition was contained the individual random effects, and all 230 *adipose CpGs* were taken forward into subsequent analyses.

CpGs influenced by the GOTO intervention correlated with expression of lipid metabolism and insulin resistance genes

The majority (n = 139, 60.4%) of the 230 *adipose CpGs* were hypermethylated following the intervention (**Fig. 3b; Supplementary Table 11**). To determine their functional potential, we annotated their genomic positions to 15 chromatin states using the adipose reference epigenome (E063) from the Roadmap Epigenomics Consortium[33]. Since the *adipose CpGs* were enriched for several repressive marks, such as polycomb repressed regions (OR = 7.76, p_{FDR} = 7.35e−43) and depleted for regulatory states, including enhancers (OR = 0.38, p_{FDR} = 1.10e−02) and active TSS (OR = 0.11, p_{FDR} = 5.21e−04), there was insufficient evidence to suggest that the *adipose CpGs* as a whole were controlling nearby transcription (**Fig. 3c; Supplementary Table 12**). Despite this, sequences within 50 bp of the *adipose CpGs* were enriched for seven known TFBS (**Fig. 3d; Supplementary Table 13**), including for four GATA family TFs involved in the initial stages of adipogenesis and obesity[50].

Although the *adipose CpGs* did not likely represent a regulatory set overall, we evaluated if individual sites correlated with changes in nearby gene expression. Within 100 kb of the 230 *adipose CpGs* there were 412 genes, and 23 of these were both differentially expressed ($p_{FDR} < 0.05$) and associated with the nearby DNAm response ($p_{FDR} < 0.05$; **Supplementary Table 14**). These 23 genes included many relevant for adipogenesis, such as *ZBTB7A51* and *ALX152* and multiple developmental genes including *EN1* and *NR2F153*. Of particular interest were *PITX2* and *DMRT3*, which were associated with responses at 3 and 16 unique *adipose CpGs*, respectively. *PITX2* encodes a TF linked to changes in fasting glucose following weight loss[54] and *DMRT3*, which associates with exercise training and diet[55,56], has been proposed as a marker of insulin resistance specifically in SAT[57].

To further investigate the importance of this set of 23 genes, we performed overrepresentation analysis and revealed enrichment for 27 terms, including many relevant to lipid metabolism and transport (e.g., Phospholipid Efflux p_{FDR} = 0.019; **Supplementary Table 15**)[58].

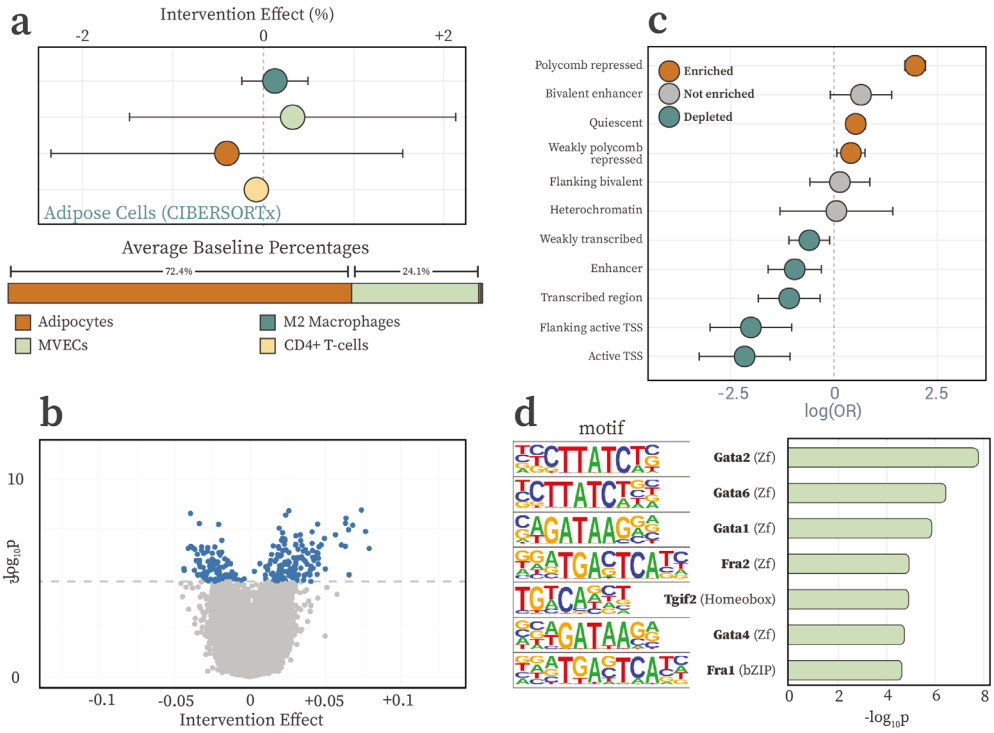

Figure 3 | Characterisation of the adipose cell counts and DNAm response to the GOTO intervention. a) Intervention effects on cell types predicted using *CIBERSORTx* alongside baseline proportions (only cells >0.5% at baseline shown) **b)** Volcano plot of the intervention effect on DNAm in SAT at over 750,000 CpGs, showing significant (blue) and non-significant (grey) CpGs. **c)** Forest plots of the OR and 95% CIs for enrichment or depletion of chromatin states using the E063 adipose reference epigenome from the Roadmap Epigenomics Consortium (four states with extremely wide CIs not shown). **d)** Bar plot of TFBS motifs enriched in sequences within 50 bp of the identified CpGs when compared to a GC-matched random genomic background.

Reductions in total body fat percentage associate with the adipose DNAm response

To link epigenetic findings in SAT to changes in health, we performed paired analyses associating DNAm effects at the *adipose CpGs* and differences in the ten health parameters shown in **Table 1 (Fig. 4a; Supplementary Table 16)**. In total, almost a third of the *adipose CpGs* (n = 75, 32.6%) associated with at least one tested trait, and more than five unique CpGs were correlated with total body fat percentage decreases (39 CpGs), adipocytokine levels (adiponectin: 8 CpGs; interleukin-6 (IL-6): 48 CpGs), BMI (12 CpGs), and WC (12 CpGs). Of these, 12 had been related to nearby gene expression in the previous analyses. Hypomethylation at two of the three *adipose CpGs* at *DMRT3* was also associated with reductions in total body fat percentage (**Fig. 4b**). Notably, these results connected DNAm effects at multiple CpGs to differential expression and improvements in health, indicating the relevance of the identified loci for physiological and molecular responses to lifestyle interventions in older adults.

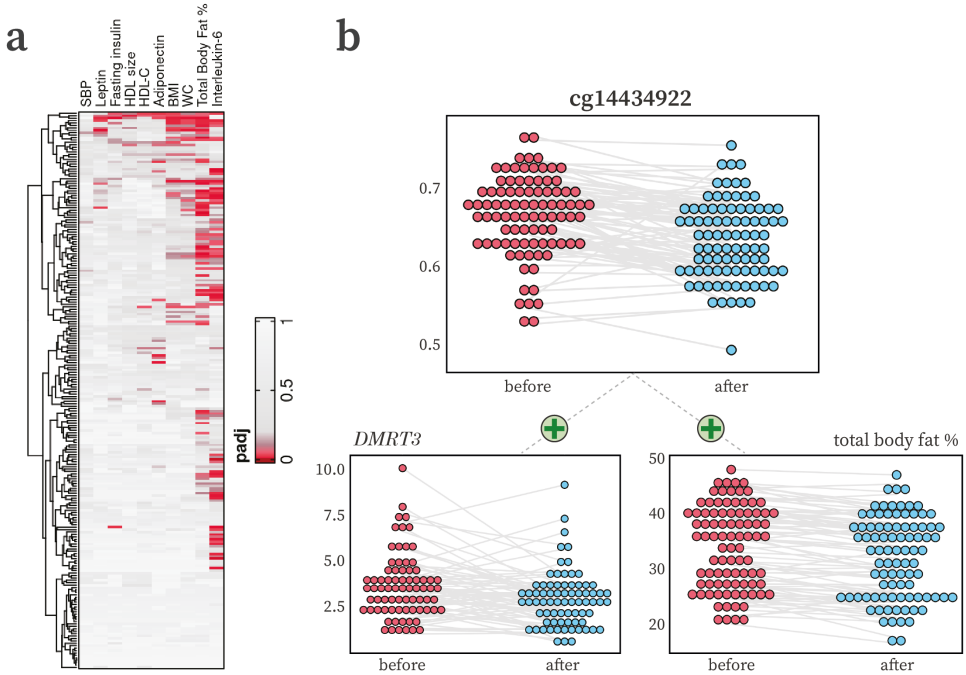

Figure 4 | Integrative analyses in subcutaneous adipose tissue (SAT). a) Clustered heatmap of association *p*-values the DNAm response at the 230 *adipose CpGs* and ten health parameters. **b)** Dot plots showing hypomethylation of DNAm in SAT at cg14434922, positively associated with decreases in adipose *DMRT3* gene expression and total body fat percentage (HDL: high density lipoprotein; SBP: systolic blood pressure; BMI: body mass index; WC: waist circumference).

Altered blood-based health parameters associate with the relatively small DNA methylation response in blood

We analysed DNAm data from paired fasted blood samples (n = 98 individuals, 196 samples), identifying 441 CpGs at distinct loci where methylation was altered following the intervention ($p_{FDR} < 0.05$), henceforth referred to as the *blood CpGs*. In cross-sectional blood-based EWAS, cell-type proportions are a well-known driver of association signals. Therefore, we extensively assessed if changes in cell types that would not be captured by the individual-level random effects existed in our data. To this end, we measured five cell types and predicted a further 36 from DNAm and gene expression data. Neutrophils and their progenitors accounted for the majority of cells (between 47.7% and 51.8% at baseline), followed by lymphocytes (36.9% to 41.1%) and monocytes (7.4% to 10.1%). There was insufficient evidence to suggest that any of the measured or predicted nucleated cell-types changed following the intervention at either the 5% nominal or FDR level. This indicated that cell-type proportions were captured by individual random effects in our models and additional adjustment would be statistically redundant (**Fig. 5a**).

In contrast to the findings in skeletal muscle and SAT, all effect sizes at the 441 b*lood CpGs* were small (β < 4%; **Fig. 5b; Supplementary Table 18**). This alone did not preclude them from functionality. To explore the likelihood that DNAm responses at the *blood CpGs* were regulatory, we performed chromatin state and TFBS enrichment analyses. This set of sites was enriched for regions flanking active TSS (OR = 1.50, p_{FDR} = 1.1e−02; **Fig. 5c; Supplementary Table 19**), although the size of this enrichment was smaller than seen in previous tissues. Sequences within 50 bp of the *blood CpGs* were enriched for three known TFBS (**Fig. 5d; Supplementary Table 20**), including NFE2L2 and MafK, TFs central to the oxidative stress response[59,60]. When we investigated genes within 100 kb of the *blood CpGs*, there were only three genes both differentially expressed and linked to nearby methylation. However, these did include two genes linked to inflammatory and immune responses (*LTBR* and *TNFRSF1A;* **Supplementary Table 21**)[61].

To explore possible distant or pleiotropic effects on health, we evaluated the association between DNAm at the *blood CpGs* and changes in the ten health parameters shown in **Table 1 (Fig. 5e; Supplementary Table 22**). Differential methylation at 66 (15.0%) of the *blood CpGs* associated with changes in nine traits, including total body fat percentage (24 CpGs), BMI (27 CpGs), WC (32 CpGs), HDL cholesterol levels (2 CpGs) and size (18 CpGs), IL-6 (3 CpGs), leptin (19 CpGs), systolic blood pressure (SBP, 2 CpGs), and fasting insulin (5 CpGs). This indicated that, despite the smaller size of the methylomic responses at the *blood CpGs* and the lack of support for *cis* regulatory effects, this set of sites was still able to mark intervention-driven improvements in immunometabolic health.

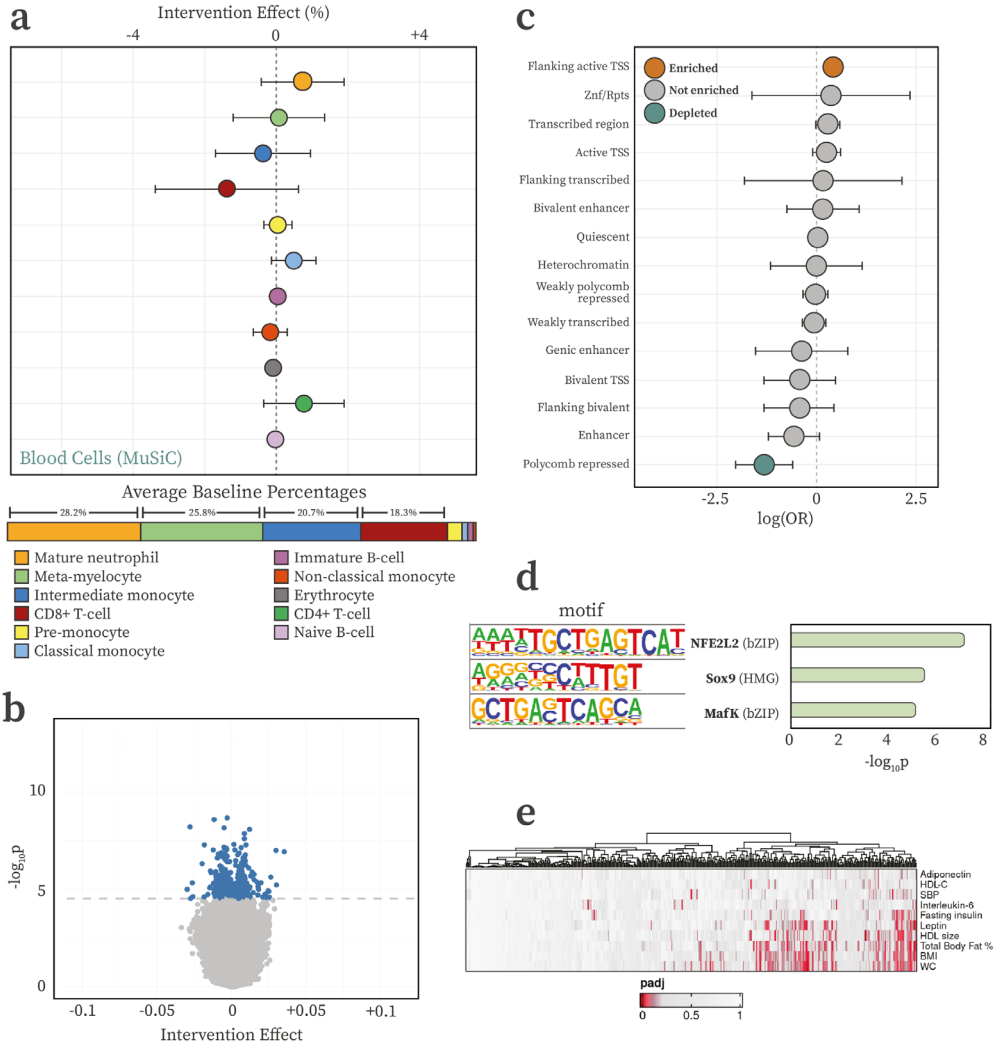

Figure 5 | Characterisation of the blood cell count and DNAm responses to the GOTO intervention. a) Intervention effects on immune cell types predicted using the IDOL algorithm alongside baseline proportions (only cells >0.5% at baseline shown). **b)** Volcano plot of the intervention effect on DNAm at over 750,000 CpGs, showing the 441 significant CpGs (blue) and nonsignificant CpGs (grey). **c)** Forest plots of the the OR and 95% CIs for enrichment (orange) or depletion (blue) of chromatin states using the E062 peripheral blood mononuclear cell (PBMC) reference epigenome. **d)** Bar plot of TFBS motifs enriched in sequences within 50 bp of identified CpGs compared to a GC-matched random genomic background. **e)** Clustered heatmap of association *p*-values between DNAm responses at the *blood CpGs* and ten health parameters.

Chronological age predictors have increased in accuracy but still capture more than just the passage of time

In the field of epigenetics and ageing, several algorithms have been developed to predict chronological age (cAge) from DNAm data. Here, we predicted cAge changes following the GOTO intervention by applying three such clocks to DNAm from pre- and post-intervention blood samples (Horvath[62], Zhang[63], and Bernabeu[64]). Correlations between actual age, which increased by 13 weeks across this longitudinal study, and predicted cAge were calculated. Predictions of cAge using Horvath, one of the original epigenetic clocks, were moderately correlated with actual age ($R = 0.730$, $p_{FDR} = 7.6e{-}34$), showing that from their inception these algorithms have performed well.

Looking at more recent clocks, we observed increases in accuracy over time with the Zhang ($R = 0.888$, $p_{FDR} = 2.7e{-}67$) and Bernabeu ($R = 0.923$, $p_{FDR} = 8.6e{-}82$) cAge predictions both correlating remarkably strongly with actual age at visit date. When looking at the predicted change in chronological age over this 13 week intervention, however, all three clocks did return a reduction in age ranging from a 22.3 week decrease (Horvath clock $p_{FDR} = 0.200$) to a 12.5 week reduction (Bernabeu $p_{FDR} = 0.155$). Overall, these results showed that cAge predictors are well correlated with and increasingly in line with actual age but still have considerably large residuals when compared to actual age. This indicated that such clocks may be swayed by other factors, such as intervention-driven health improvements, and could benefit from further refinement if their intention is to predict calendar age.

GrimAge captured the effect of the GOTO intervention and associated with metabolic and physiological health improvements

In contrast to cAge estimates, recent biological age (bAge) predictors are commonly trained on a combination of age, health parameters, and mortality data. We investigated four bAge clocks (Bernabeu[64], grimAge[65], phenoAge[66], and MEAT[67]). The first three of these were trained using blood samples, and thus we used blood-based DNAm from before and after the GOTO intervention as input. The fourth clock (MEAT) was a muscle-specific algorithm and so was applied to DNAm data from the muscle samples instead. Using a paired analysis, we estimated the effect of the GOTO intervention on biological age, adjusting for age, sex, and technical covariates (**Fig. 6a; Supplementary Table 23**).

All four clocks predicted a decrease in bAge following the GOTO intervention with estimates ranging from a 16.1-week decrease (Bernabeu $p_{FDR} = 2.4e{-}01$) to a 57.9-week decrease (MEAT $p_{FDR} = 2.1e{-}02$). After adjusting for multiple testing, however, only decreases in grimAge ($\beta = -34.6$ weeks, $p_{FDR} = 1.4e{-}04$) and MEAT ($\beta = -57.9$ weeks, $p_{FDR} = 2.1e{-}02$) remained significant at the 5% level. Considering that the strongest methylation

response to GOTO was in muscle, these results supported the development of tissue-specific algorithms for bAge prediction in epigenomic studies. Additionally, since grimAge is established as strongly associated with frailty risk as compared with other epigenetic age measures[68], this finding highlighted differences in available algorithms and supported a specific relevance for grimAge to ageing populations.

To explore whether observed reductions in bAge were connected to immunometabolic health improvements, we associated changes in bAge clocks with significant effects with the ten metabolic health parameters shown in **Table 1 (Supplementary Table 24)**. Seven of the ten tested traits were significantly associated with grimAge at the 5% level after adjusting for multiple testing, including BMI (β = 0.30, p_{FDR} = 5.2e−03), total body fat percentage (β = 0.10, p_{FDR} = 3.9e−02), and leptin levels (β = 0.08, p_{FDR} = 1.3e−02). The directions of effect consistently connected decreasing bAge to improved immunometabolic health (**Fig. 6b**). Together, these results showcased the power of blood-based DNAm markers and bAge algorithms to capture health improvements following lifestyle interventions in older adults.

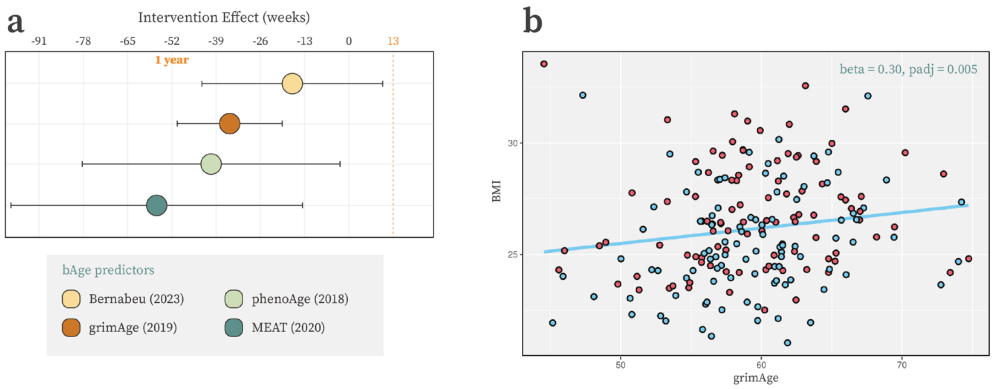

Figure 6 | The GOTO intervention reduces measures of epigenetic age. a) Predicted decreases in biological age following GOTO for four modern bAge algorithms. **b)** Scatter plot showing the association between grimAge and observed BMI both before (red) and after (blue) the GOTO intervention.

Discussion

Tissue-specific DNA methylation responses in muscle, adipose, and blood tissues

Following a 13-week combined lifestyle intervention, we observed DNAm responses at 162 CpGs in skeletal muscle, 230 CpGs in SAT, and 441 CpGs in fasted blood. We characterised the regulatory nature of these responsive CpGs, detecting enrichments for active chromatin states and relevant TFBS. Using matched gene expression and health parameter data, we performed integrative analyses and uncovered relationships between epigenetic changes and metabolic health, with links to insulin sensitivity, muscle regeneration potential, and body composition. On a molecular level, the directions of DNAm responses corresponded with previously observed transcriptomic effects in this study[69]. In skeletal muscle, identified CpGs were predominantly hypomethylated, an established effect of physical activity[70] and aligning with increases in gene expression in muscle. In contrast, methylation increased in SAT, tying in with global decreases in gene expression observed in this tissue. Lastly, in blood, the signal was small in both the methylome and the transcriptome[27,69], possibly due to molecular changes in blood lying further from functionally responding tissues and representing diffuse or systemic alterations.

RNA-Seq data was available to investigate *cis* associations between differentially expressed genes and DNAm responses in the three tissues. In skeletal muscle, expression changes at 71 genes in close proximity to identified CpGs were associated with differential methylation. In contrast, 23 genes were linked to DNAm changes in SAT and only three genes had clear *cis* correlations with CpGs in blood. Looking at the function of the genes identified in muscle and SAT, many were connected to insulin sensitivity and glucose uptake in relevant cell types. This included *GRB10*[42,43], which directly binds to and regulates insulin receptors, *PLEKHG4*[39–41], which is implicated in the translocation of GLUT4 transporters to the membrane in skeletal muscle cells, and *DMRT3*[71], an insulin sensitivity marker specific to SAT. In particular, the lowered expression of *GRB10* observed here enhances insulin-induced PI3K/Akt signalling and glucose uptake in myotubes and increases muscle size[42,70,72,73]. Changes in fasting insulin levels were also associated with DNAm responses in all three tissues (muscle: 2 CpGs, SAT: 3 CpGs; blood: 5 CpGs), although there was no overlap with the identified genes. Caloric restriction and exercise have established effects on insulin resistance with consequences for immunometabolic health, and this study outlined potential molecular mechanisms behind these effects[74–76].

We also observed enrichments for regulatory chromatin states in muscle and blood, including for enhancers and regions flanking active TSS. Relevant TFBS were additionally enriched in sequences within 50 bp of the differentially methylated CpGs in all three tissues. In muscle, we identified Fos and JunB binding sites close to responsive CpGs, TFs with established relevance for muscle health[36]. In SAT, binding sites of four

known GATA family TFs were enriched, pointing to transcriptional regulators connected to adipose tissue remodelling[50]. Since DNAm elicits functional effects by modulating the accessibility of regulatory sites, these findings strengthened the hypothesis that observed DNAm changes were regulatory and may have had functional effects on nearby gene expression[34].

Differential methylation links to metabolic health and decreases in epigenetic age

The GOTO intervention imparted a metabolic health benefit on the study population[25,26], and these improvements also tracked with DNAm adaptations. At over half of the *muscle CpGs* and almost a third of the *adipose CpGs,* DNAm responses were associated with alterations in one or more health parameters. Exemplifying this, DNAm in all three tissues could be connected to eight of the ten tested traits, including total body fat percentage (blood: 24 CpGs, adipose: 39 CpGs, muscle: 13 CpGs), leptin (blood: 19 CpGs, adipose: 4 CpGs, muscle: 14 CpGs), and BMI (blood: 27 CpGs, adipose: 12 CpGs, muscle: 7 CpGs). Favourable changes in body composition, as seen in the GOTO intervention study, are associated with a more balanced secretion of adipokines from adipose tissue, decreasing the risk of insulin resistance and type 2 diabetes. We show here that DNAm responses were associated with key measures of such a reduction in immunometabolic risk.

Previous investigations into the health benefits of the GOTO intervention have demonstrated sex-specific effects, possibly as a result of physiological differences between sexes and the personalised nature of the protocol. Sex-specific differences in muscle performance are partly attributed to larger proportions of type-I fibres in women, characterised by slower oxidative metabolism[77]. However, in this study where we investigated effects at over 750,000 CpGs across the epigenome, we did not consider the two sexes separately. In the future, it will be important to uncover the molecular mechanisms behind observed disparities between men and women using studies more suitably powered for sex stratification.

Lastly, we calculated cAge and bAge in blood and muscle samples using available algorithms[62–67]. These highlighted the impressive precision and accuracy of current epigenetic clocks for calendar age prediction, with estimates from a recent model highly correlated with actual age (R = 0.923)[64]. Yet, all tested cAge algorithms still reported age reductions following the intervention despite participants ageing by 13 weeks. It is plausible, therefore, that these cAge estimates are influenced by other factors such as immunometabolic health improvements. To investigate this further, we evaluated if bAge predictors captured the health benefits of the GOTO intervention. All four algorithms returned a decrease in bAge ranging from −16.1 weeks to −57.9 weeks, larger than the previous cAge estimates. The muscle-specific MEAT algorithm represented the greatest effect and it, alongside reductions in bAge as predicted by grimAge, were

still significant at the 5% level after adjusting for multiple testing. GrimAge, in particular, was associated with observed improvements in seven of the 10 tested health parameters, including BMI, circulating leptin levels, and total body fat percentage. GrimAge and the metabolomics-based score, MetaboHealth, have both previously been reported as good measures of health improvements[69], frailty[68], and mortality[65,78]. The beneficial shifts observed here in these scores indicate potentially global and long-term health improvements from the GOTO intervention protocol, and also highlight the possible value of molecular algorithms for monitoring intervention effects both in general, and specifically in older populations.

It is important to note that this intervention was carried out in healthy, older adults. For some older individuals, for example those with a risk of sarcopenia, this mild intervention may not be the most optimal regime. Other protocols, including ProMuscle and a novel upcoming study VOILA, are better focused on improving muscle mass and strength by including resistance training, increased protein intake, or protein supplementation[79,80]. Clinical study populations of older individuals may also require other response markers due to the higher levels of acute inflammatory proteins in population-based elderly.

Overall, our in-depth study of the methylome, transcriptome, and phenome exemplifies the biological changes that older adults experience following a mild intervention, such as GOTO. The absence of any overlap between the identified sets of CpGs demonstrates strong tissue-specificity in our findings and this, coupled with the distinct directional differences (hypermethylation in adipose tissue and hypomethylation in muscle), highlights the importance of using a multi-tissue approach when investigating the influence of environmental changes on the methylome. As DNAm represents only one form of epigenetic control, more in-depth interpretation of these findings may require examination of other layers of the epigenome, such as chromatin accessibility using ATAC-seq.

This study established the methylomic responses to a 13-week lifestyle intervention in older adults in both circulating cells and relevant metabolic tissues. We identified differential methylation at CpGs located in regulatory regions in close proximity to TFBS. Effects at these CpGs were associated with differential expression of insulin sensitivity genes, including *GRB10* in muscle and *DMRT3* in adipose, and with imparted metabolic health benefits. Identified loci may be investigated to monitor immunometabolic risk, progression of disease, and response to treatment in the future. The GOTO response was also represented by four epigenomic bAge markers and GrimAge, in particular, was able to capture the health improvements imparted to the participants. This study further demonstrated the importance of collecting biologically relevant tissues in intervention studies and highlighted how modifiable molecular markers can capture health improvements following lifestyle changes in older people.

Methods

Recruitment

The GOTO study was nested within the Leiden Longevity Study, a longitudinal cohort of long-lived Caucasian siblings, their offspring, and partners thereof. The GOTO study recruited healthy, older (mean age 63 years) adults (n = 164) between June 2012 and April 2013[25]. Individuals between 46 and 75 years with a BMI between 23 and 35 kg/m^2 from the pool of offspring and partners were eligible for the study.

Exclusion criteria included being on diabetic medication (for type 1 or 2 diabetes), having high fasting blood glucose levels (≥7.0 mmol/L), recent weight change (≥3 kg in the past 6 months), engagement in heavy or intensive physical activity (top sport or physically heavy work), any disease or condition that seriously affected body weight and/or body composition, recent immobilization (for over 1 week in the last 3 months), psychiatric or behavioural problems, use of thyroid medication or immunosuppressive drugs, concurrent participation in any other intervention studies or weight management programs, or not being registered with a general practitioner.

Intervention protocol

Expanding on the combined lifestyle arm of the CALERIE (Comprehensive Assessment of Long-term Effects of Reducing Intake of Energy) study, GOTO participants reduced their energy balance by 25% for 13 weeks, through a combination of caloric restriction and increased physical activity[6]. Informed by baseline questionnaires on energy intake (150-item food frequency questionnaire) and expenditure (IPAQ-SF, International Physical Activity Questionnaire Short Form), dieticians and physiotherapists prescribed individual guidelines to achieve the intervention. Participants were advised to increase physical activity in a way that was compatible with their lifestyle, and dietary guidelines aimed to follow the Dutch Guidelines for a Healthy Diet (2006).

To check and stimulate adherence to the intervention, there was weekly contact with both the dietician and physiotherapist. Participants recorded their adherence to the intervention plan in a diary, and two 24-hour recalls were performed during the first and last month of the intervention. Days of the recall were unannounced to the participants and randomised to obtain a good distribution of weekdays and weekends. During monthly home visits, body weight and composition were measured.

Sample collection

Both prior and post intervention, blood (95 mL) was drawn by venepuncture between 8 and 9 a.m. in the hospital after at least 10 hours of fasting. The participants consumed a SLM Nutridrink TM[72] representative of a typical Northern European meal (300 kcal: 35% energy from fat, 50% from carbohydrate, and 16% protein) between 9 a.m. and noon on the same day. Following this, skeletal muscle biopsies were taken from the musculus vastus lateralis and a subcutaneous adipose biopsy was taken from the abdomen. Biopsies were taken under local anaesthetic and immediately frozen in liquid nitrogen before being stored at −80°C for subsequent analysis.

Of the 164 individuals in the GOTO study, we profiled DNAm from 104 individuals at both timepoints for multiple tissues (sample n = 562). All 562 samples represented distinct samples from a unique timepoint, individual, and tissue combination and not duplicates. DNA from whole blood (n = 206) was isolated using QIAmp DNA Mini kits (QIAgen) and using NucleoMag Tissue kits (Machery Nagel) for adipose (n = 188) and muscle (n = 168) samples. Pairs of samples were shuffled and plated so that they would be adjacent on the same array. These pairs were randomised across eight 96-well plates by tissue, age, and sex using *Omixer*, and sent for profiling using the Infinium MethylationEPIC Kit (Illumina, Helmholtz Institute)[81].

DNA methylation profiling

Following receipt of the methylation data, preprocessing and quality control (QC) followed the *DNAmArray* pipeline[82]. *MethylAid* plots were used to visualize and check sample quality[83]. Due to technical issues with three of the Infinium MethylationEPIC arrays, 25 samples failed quality control checks. These alongside their pairs (n = 30) were removed from the data, and 24 samples with sufficient remaining material were reprofiled and subsequently passed QC checks.

After combining data from both waves, tissue identity was confirmed with PC analysis (PCA) plots, and four outlying samples and their pairs (n = 8) were removed. Sample mismatches were detected and resolved by comparing genotype data with DNAm-derived genotypes using *omicsPrint*[84]. Individuals (n = 6) identified from diary data as non-compliers were also removed. Lastly, methylation-predicted sex was used as a final check of sample identity.

The data underwent functional normalization using four PCs, followed by removal of outlying or unreliable values, such as those based on low bead number (0.20%), intensity (0.08%), that were not distinguishable from background noise (0.37%), or more than 3 interquartile ranges from the nearest quartile per CpG (0.28%). Any probes or samples with over 5% missingness were removed (0.00% of samples, 1.06% of CpGs). Additionally, cross-reactive, polymorphic[85], poorly reproducible[86], blacklisted[87], and sex chromosomal probes were removed. The resulting dataset contained DNAm data at 755,777 CpGs from 534 samples (196 blood, 178 adipose, and 160 muscle) from 102 individuals. For 66 individuals (64.7%), there was complete data from all three tissues at both timepoints.

RNA sequencing

RNA isolation and sequencing has been described previously[69]. In short, libraries were prepared using Illumina TruSeq version 2 library preparation kits. Data processing was performed using the in-house BIOPET Gentrap pipeline[88]. The following steps were part of the data processing: low quality trimming using sickle version 12.00. Cutadapt version 1.1 was used to perform the adapter clipping. The reads were aligned to GRCh37 while masking for single nucleotide polymorphisms common in the Dutch population (Genome of the Netherlands (GoNL) 45 minor allele frequency > 0.01), using STAR version 2.3.0e. Picard version 2.4.1. was used to perform sam to .bam conversion and sorting. Read quantification was performed using htseq-count version 0.6.1.p1 using Ensembl gene annotations version 86 for gene definitions. In blood, the sequencing resulted in an average of 37.2 million reads per sample, of which 97% (±0.4%) were mapped. In SAT, samples had an average of 11.4 million sequenced reads, of which 95% (±1.6%) were mapped. In muscle, an average of 36.9 million sequence reads per sample, of which 98% (±0.4%) were mapped.

Cell-type proportions

In muscle, nuclei types were predicted using the MuSiC algorithm combined with publicly available single nuclei reference transcriptomes and bulk expression data[30,31]. For subcutaneous adipose samples, no suitable single cell reference transcriptome was available. Therefore, adipose cell types were predicted using CIBERSORTx and a publicly available signature matrix provided from studies in TwinsUK and GTEx[48,49]. In fasted blood, the percentage of cell types (neutrophils, lymphocytes, monocytes, eosinophils, and basophils) was measured with a differential test. To investigate the intervention effect on specific immune cell subtypes, we combined a single cell reference atlas with whole blood expression data and the MuSiC algorithm estimating 32 different cell types[30,89]. Furthermore, the Identifying Optimal Libraries (IDOL) and IDOL-extended algorithms deconvoluted six and twelve subtypes from the DNAm data, respectively[90,91].

Statistical analysis

For all statistical investigations, *p*-values were adjusted for multiple testing using the FDR method, and significance was assessed at the 5% level. Intervention effects on DNAm were evaluated using mixed models, with a fixed effect for the intervention (time), an individual random effect (ID), and adjustment for confounders (age, sex, and smoking), technical covariates (plate and array row), and the first five PCs:

$$DNAm_{ijk} \sim time_{ij} + age_i + sex_i + smoke_i + plate1_{ij} + \cdots + plate10_{ij} + arrayRow_{ij} + PC1_{ij} + \cdots + PC5_{ij} + (1|ID_i)$$

Muscle models were additionally adjusted for predicted endothelial nuclei proportions. Bias and inflation in the test statistics was inspected and adjusted for using the Bioconductor package, *bacon*, with default priors ($\alpha = 1.28$, $\beta = 0.36$)[92].

CpG interpretation

Differentially methylated regions To assess the number of distinct genomic loci in our results, differentially methylated regions (DMRs) were calculated using the *DMRfinder* algorithm as implemented in the *DNAmArray* workflow[82,93]. DMRs were defined as regions with at least three differentially methylated probes (DMPs) with an inter-CpG distance less than 1 kb, allowing a maximum of three non-DMPs across a DMR. The number of distinct loci was the total number of DMPs minus the number of DMPs in DMRs plus the number of DMRs called by DMRfinder.

Chromatin state enrichment FDR-significant CpGs were annotated to chromatin states using appropriate reference epigenomes from the Roadmap Epigenomics Consortium (E062 for blood, E063 for adipose, E107 and E108 for muscle)[33]. Logistic regressions models were fitted using the *glm* function in R for each of the 15 chromatin states to assess if the number of significant CpGs annotated to that chromatin state differed significantly from the set of tested CpGs.

TFBS enrichment A 50 bp window around identified CpGs was scanned for enrichment of known motifs compared to background noise matched for GC content using *findMotifsGenome.pl* from HOMER[94]. ENCODE TFBS annotation for TFs and CpGs on the EPIC array was further used to investigate the size of binding sites and distance from CpG to summit[85].

Gene annotation Genomic locations of human transcripts, exons, coding sequences, and genes were imported from the Ensembl database using *makeTxDbFromEnsembl* from the GenomicFeatures Bioconductor package[95]. These both annotated CpGs to their nearest gene and identified all genes within 100 kb of each site.

Differential gene expression Gene expression changes were analysed as described previously but with both sexes combined in a single analysis[69]. Briefly, the differential gene expression analysis used linear mixed models in combination with voom normalization. Models were adjusted for technical factors, age, and sex as fixed effects and included a random effect for ID.

Expression quantitative trait methylation The association between DNAm and differentially expressed genes within 100 kb was investigated using available expression and methylation data. Lowly expressed genes were removed and $\log_2$CPM values were calculated. For each gene, we applied RIN transformations as described previously[96].

$$DNAm_{ij} \sim gene_{ij} + age_i + sex_i + smoke_i + plate1_{ij} + \cdots + plate10_{ij} + arrayRow_{ij} + flowcell_{ij} + (1|ID_i)$$

Over-representation analysis The list of candidate target genes (differentially expressed genes associated with a DNAm response within 100kb) was used as input for over-representation analysis in *clusterProfiler*, combined with recent (updated in the last 6 years) databases relating to human health and disease downloaded from Enrichr (GO Biological Process 2023, KEGG Human 2021, and Reactome 2022)[58].

Health parameter associations Linear mixed models were used to investigate the association between DNAm and ten health parameters, adjusting for age, sex, smoking, technical covariates:

$$DNAm_{ij} \sim trait_{ij} + age_i + sex_i + smoke_i + plate1_{ij} + \cdots + plate10_{ij} + arrayRow_{ij} + (1|ID_i)$$

Epigenetic clock algorithms

cAge prediction Using the *dnaMethyAge* package[97], Horvath[62], Zhang[63], and Bernabeu[64] based cAge was predicted. Correlations between these estimates and actual age was assessed using a Pearson's correlation test with the *cor.test* function in R.

bAge prediction Using the *dnaMethyAge* package[97], LevineM2018 (PhenoAge) was predicted[66]. grimAge was estimated using the coefficients, R, and Python scripts provided by the researchers who developed this measure[65]. Bernabeu's bAge[64] was predicted by combining grimAge, DNAm data, and phenotype data in the *bage_predictor.R* script provided on their GitHub (`elenabernabeu/cage_bage`). Lastly, MEAT bAge[67] was predicted from muscle DNAm data using the MEAT Bioconductor package for R. For all bAge predictions, paired analyses estimated changes following the GOTO intervention, adjusting for age, sex, technical covariates and with a random effect for ID:

$$bAge_{ij} \sim time_i + age_i + sex_i + plate1_{ij} + \cdots + plate10_{ij} + arrayRow_{ij} + (1|ID_i)$$

Associations with health parameters Associations between grimAge and ten health parameters were investigated using a paired analysis, adjusting for age, sex, technical covariates, and with a random effect for ID:

$$grimAge_{ij} \sim trait_{ij} + age_i + sex_i + plate1_{ij} + \cdots + plate10_{ij} + arrayRow_{ij} + (1|ID_i)$$

Ethics statement

The Growing Old TOgether Study protocol was approved by the Medical Ethical Committee of the Leiden University Medical Center before the start of the study (P11.187). In accordance with the Declaration of Helsinki, the Growing Old TOgether Study obtained informed consent from all participants prior to their entering the study. This trial was registered at the Dutch Trial Register (https://onderzoekmetmensen.nl/en) as GOT NL3301.

Author contributions

P.E.S. and C.d.G. designed the study. M.B. collected and curated the health data. N.L. and E.S. generated the DNAm and transcriptome data. L.S., B.T.H., M.B., and P.E.S. designed the data analysis approach, L.S. and F.A.B. performed data analysis, I.M. and L.S. performed the cell deconvolution analyses, D.B. provided expertise on epigenetic clocks, Y.R., A.B., G.B-B., and C.T. provided expertise on muscle physiology, M.W. profiled DNAm in the three tissues and provided vital intellectual contributions, and L.S., Y.R., A.B., G.B-B., C.T., B.T.H., P.E.S., and M.B. performed the research and interpreted the data. All authors were involved in drafting and revising the manuscript.

Funding

The research leading to these results was supported by the Joint Programming Initiative "a Healthy Diet for a Healthy Life" (JPI-HDHL) DIMENSION project (ZonMW project number: 529051021) and ZonMW Project VOILA (ZonMW project number: 457001001). The underlying intervention study was financially supported by the Netherlands Consortium for Healthy Ageing (grant 050-060-810), in the framework of the Netherlands Genomics Initiative, Netherlands Organization for Scientific Research (NWO) and by BBMRI-NL, a Research Infrastructure financed by the Dutch government (NWO 184.021.007). The funding agencies had no role in the design and conduct of the study; collection, management, analysis, and interpretation of the data; and preparation, review, or approval of the manuscript.

Declarations of interest

The authors declare no competing interests.

Data & code availability

Data supporting the findings of this study are accessible upon reasonable request to the corresponding author. The individual-level data are not publicly available due to privacy or ethical restrictions. All other data used in this study are publicly available: reference epigenomes are available from the Roadmap Epigenomics Consortium[33] and TFBS data is available within the HOMER software[94]. All the software and programmes used to conduct these analyses are freely available. Scripts used during this analysis are provided on GitHub at `nebulyra.github.io/goto_dnam`.

References

1. Fiuza-Luces, C. *et al.* Exercise is the real polypill. *Physiology* **28** (5): 330-358 (2013).
2. Knowler, W. C. *et al.* Reduction in the incidence of type 2 diabetes with lifestyle intervention or metformin. *N Engl J Med* **346** (6): 393-403 (2002).
3. The Diabetes Prevention Program (DPP): Description of lifestyle intervention. *Diabetes Care* **25** (12): 2165-2171 (2002).
4. Zhang, Y. *et al.* Combined lifestyle factors and risk of incident type 2 diabetes and prognosis among individuals with type 2 diabetes: a systematic review and meta-analysis of prospective cohort studies. *Diabetologia* **63** (1): 21-33 (2020).
5. Leitner, D. R. *et al.* Obesity and type 2 diabetes: Two diseases with a need for combined treatment strategies - EASO can lead the way. *Obes Facts* **10** (5): 483-492 (2017).
6. Kraus, W. E. *et al.* 2 years of calorie restriction and cardiometabolic risk (CALERIE): exploratory outcomes of a multicentre, phase 2, randomised controlled trial. *Lancet Diabetes Endocrinol* **7** (9): 673-683 (2019).
7. Eriksson, J. *et al.* Prevention of Type II diabetes in subjects with impaired glucose tolerance: The Diabetes Prevention Study (DPS) in Finland. Study design and 1-year interim report on the feasibility of the lifestyle intervention programme. *Diabetologia* **42** (7): 793–801 (1999).
8. Voisin, S. *et al.* Exercise training and DNA methylation in humans. *Acta Physiologica* **213** (1): 39-59 (2015).
9. van der Harst, P., de Windt, L. J. *and* Chambers, J. C. Translational Perspective on Epigenetics in Cardiovascular Disease. *J Am Coll Cardiol* **70** (5): 590-606 (2017).
10. Gevaert, A. B. *et al.* Epigenetics in the primary and secondary prevention of cardiovascular disease: influence of exercise and nutrition. *Eur J Prev Cardiol* **29** (17): 2183-2199 (2022).
11. Nakajima, K. *et al.* Exercise effects on methylation of ASC gene. *Int J Sports Med* **31** (9): 671-675 (2010).
12. Butts, B. *et al.* Effects of Exercise on ASC Methylation and IL-1 Cytokines in Heart Failure. *Med Sci Sports Exerc* **50** (9): 1757-1766 (2018).

13. Ma, J. *et al.* Whole Blood DNA Methylation Signatures of Diet Are Associated With Cardiovascular Disease Risk Factors and All-Cause Mortality. *Circ Genom Precis Med* **13** (4): E002766 (2020).
14. Keller, M. et al. DNA methylation signature in blood mirrors successful weight-loss during lifestyle interventions: the CENTRAL trial Genome Med 12: 97 (2020).
15. Stanford, K. I. & Goodyear, L. J. Muscle-Adipose Tissue Cross Talk. Cold Spring Harb Perspect Med 8, a029801 (2018).
16. Jacobsen, S. C. et al. Effects of short-term high-fat overfeeding on genome-wide DNA methylation in the skeletal muscle of healthy young men. Diabetologia 55, 3341–3349 (2012).
17. Barrès, R. et al. Acute exercise remodels promoter methylation in human skeletal muscle. Cell Metab 15, 405–411 (2012).
18. Rönn, T. et al. A Six Months Exercise Intervention Influences the Genome-wide DNA Methylation Pattern in Human Adipose Tissue. PLoS Genet 9, (2013).
19. Gillberg, L., Jacobsen, S. C., Rönn, T., Brøns, C. & Vaag, A. PPARGC1A DNA methylation in subcutaneous adipose tissue in low birth weight subjects - Impact of 5 days of high-fat overfeeding. Metabolism 63, 263–271 (2014).
20. Fabre, O. et al. Exercise training alters the genomic response to acute exercise in human adipose tissue. Epigenomics 10, 1033–1050 (2018).
21. Savikj, M. et al. Exercise timing influences multi-tissue metabolome and skeletal muscle proteome profiles in type 2 diabetic patients – A randomized crossover trial. Metabolism 135, (2022).
22. Moore, T. M. et al. Conserved multi-tissue transcriptomic adaptations to exercise training in humans and mice. Cell Rep 42, (2023).
23. Mill, J. & Heijmans, B. T. From promises to practical strategies in epigenetic epidemiology. Nat Rev Genet 14, 585–594 (2013).
24. Rickman, A. D. et al. The CALERIE Study: Design and methods of an innovative 25% caloric restriction intervention. Contemp Clin Trials 32, 874–881 (2011).
25. van de Rest, O. et al. Metabolic effects of a 13-weeks lifestyle intervention in older adults: The Growing Old Together Study. Aging 8, 111–126 (2016).
26. Beekman, M. et al. Lifestyle-Intervention-Induced Reduction of Abdominal Fat Is Reflected by a Decreased Circulating Glycerol Level and an Increased HDL Diameter. Mol Nutr Food Res 64, (2020).
27. Gehrmann, T. et al. A Combined Lifestyle Intervention Induces a Sensitization of the Blood Transcriptomic Response to a Nutrient Challenge. Aging Biology 2, 20240036 (2024).
28. Bogaards, F. A. et al. Secondary integrated analysis of multi-tissue transcriptomic responses to a combined lifestyle intervention in older adults from the GOTO nonrandomized trial. Nat Commun 15, (2024).
29. Bogaards, F. A. et al. PLIS: A metabolomic response monitor to a lifestyle intervention study in older adults. FASEB Journal 36, (2022).
30. Wang, X., Park, J., Susztak, K., Zhang, N. R. & Li, M. Bulk tissue cell type deconvolution with multi-subject single-cell expression reference. Nat Commun 10, (2019).
31. Perez, K. et al. Single nuclei profiling identifies cell specific markers of skeletal muscle aging, frailty, and senescence. Aging 14, 9393–9422 (2022).
32. Kwak, S.-E., Lee, J.-H., Zhang, D. & Song, W. Angiogenesis: focusing on the effects of exercise in aging and cancer. J Exerc Nutrition Biochem 22, 21–26 (2018).
33. Roadmap Epigenomics Consortium et al. Integrative analysis of 111 reference human epigenomes. Nature 2015 518:7539 518, 317–330 (2015).
34. Kaluscha, S. et al. Evidence that direct inhibition of transcription factor binding is the prevailing mode of gene and repeat repression by DNA methylation. Nat Genet 54, 1895–1906 (2022).
35. Trenerry, M. K., Carey, K. A., Ward, A. C. & Cameron-Smith, D. STAT3 signaling is activated in human skeletal muscle following acute resistance exercise. J Appl Physiol 102, 1483–1489 (2007).
36. Puntschart, A. et al. Expression of fos and jun genes in human skeletal muscle after exercise. Am J Physiol Cell Physiol 274, (1998).
37. Galvagni, F., Cantini, M. & Oliviero, S. The utrophin gene is transcriptionally up-regulated in regenerating muscle. Journal of Biological Chemistry 277, 19106–19113 (2002).
38. Almada, A. E. et al. FOS licenses early events in stem cell activation driving skeletal muscle regeneration. Cell Rep 34, 108656 (2021).
39. Machin, P. A., Tsonou, E., Hornigold, D. C. & Welch, H. C. E. Rho family gtpases and rho gefs in glucose homeostasis. Cells 10, (2021).
40. Ha, N. T. & Lee, C. H. Roles of farnesyl-diphosphate farnesyltransferase 1 in tumour and tumour microenvironments. Cells 9, 1–33 (2020).
41. Shrestha, M. M., Lim, C. Y., Bi, X., Robinson, R. C. & Han, W. Tmod3 Phosphorylation Mediates AMPK-Dependent GLUT4 Plasma Membrane Insertion in Myoblasts. Front Endocrinol (Lausanne) 12, (2021).
42. Holt, L. J. et al. Ablation of Grb10 Specifically in Muscle Impacts Muscle Size and Glucose Metabolism in Mice. Endocrinology 159, 1339–1351 (2018).

43. Edick, A. M., Auclair, O. & Burgos, S. A. Role of Grb10 in mTORC1-dependent regulation of insulin signaling and action in human skeletal muscle cells. Am J Physiol Endocrinol Metab 318, E173–E183 (2020).
44. Raz, Y. et al. A data-driven methodology reveals novel myofiber clusters in older human muscles. FASEB Journal 34, 5525–5537 (2020).
45. Azhar, M., Wardhani, B. W. K. & Renesteen, E. The regenerative potential of Pax3/Pax7 on skeletal muscle injury. Journal of Genetic Engineering and Biotechnology 20, (2022).
46. Snijders, T., Holwerda, A. M., van Loon, L. J. C. & Verdijk, L. B. Myonuclear content and domain size in small versus larger muscle fibres in response to 12 weeks of resistance exercise training in older adults. Acta Physiologica 231, (2021).
47. Hansson, K. A. et al. Myonuclear content regulates cell size with similar scaling properties in mice and humans. Nat Commun 11, (2020).
48. Newman, A. M. et al. Determining cell type abundance and expression from bulk tissues with digital cytometry. Nat Biotechnol 37, 773–782 (2019).
49. Glastonbury, C. A., Couto Alves, A., El-Sayed Moustafa, J. S. & Small, K. S. Cell-Type Heterogeneity in Adipose Tissue Is Associated with Complex Traits and Reveals Disease-Relevant Cell-Specific eQTLs. Am J Hum Genet 104, 1013–1024 (2019).
50. Tong, Q. et al. Function of GATA transcription factors in preadipocyte-adipocyte transition. Science (1979) 290, 134–138 (2000).
51. Laudes, M. et al. Role of the POZ Zinc Finger Transcription Factor FBI-1 in Human and Murine Adipogenesis. Journal of Biological Chemistry 279, 11711–11718 (2004).
52. Breitfeld, J. et al. Developmentally Driven Changes in Adipogenesis in Different Fat Depots Are Related to Obesity. Front Endocrinol (Lausanne) 11, (2020).
53. Singh, S., Rajput, Y. S., Barui, A. K., Sharma, R. & Grover, S. Expression of developmental genes in brown fat cells grown in vitro is linked with lipid accumulation. In Vitro Cell Dev Biol Anim 51, 1003–1011 (2015).
54. Macartney-Coxson, D. et al. Genome-wide DNA methylation analysis reveals loci that distinguish different types of adipose tissue in obese individuals. Clin Epigenetics 9, (2017).
55. Nono Nankam, P. A. et al. Distinct abdominal and gluteal adipose tissue transcriptome signatures are altered by exercise training in African women with obesity. Sci Rep 10, 10240 (2020).
56. Divoux, A. et al. DNA Methylation as a Marker of Body Shape in Premenopausal Women. Front Genet 12, 709342 (2021).
57. Clemente-Olivo, M. P. et al. Four-and-a-half LIM domain protein 2 (FHL2) deficiency protects mice from diet-induced obesity and high FHL2 expression marks human obesity. Metabolism 121, (2021).
58. Wu, T. et al. clusterProfiler 4.0: A universal enrichment tool for interpreting omics data. Innovation 2, (2021).
59. Ryoo, I. geun & Kwak, M. K. Regulatory crosstalk between the oxidative stress-related transcription factor Nfe2l2/Nrf2 and mitochondria. Toxicol Appl Pharmacol 359, 24–33 (2018).
60. Hwang, Y. J. et al. MafK positively regulates NF-κB activity by enhancing CBP-mediated p65 acetylation. Sci Rep 3, (2013).
61. Piao, W. et al. LTβR Signaling Controls Lymphatic Migration of Immune Cells. Cells 10, 747 (2021).
62. Horvath, S. DNA methylation age of human tissues and cell types. Genome Biol 14, (2013).
63. Zhang, Q. et al. Improved precision of epigenetic clock estimates across tissues and its implication for biological ageing. Genome Med 11, 54 (2019).
64. Bernabeu, E. et al. Refining epigenetic prediction of chronological and biological age. Genome Med 15, 1–15 (2023).
65. Lu, A. T. et al. DNA methylation GrimAge strongly predicts lifespan and healthspan. Aging 11, 303–327 (2019).
66. Levine, M. E. et al. An epigenetic biomarker of aging for lifespan and healthspan. Aging 10, 573–591 (2018).
67. Voisin, S. et al. An epigenetic clock for human skeletal muscle. J Cachexia Sarcopenia Muscle 11, 887–898 (2020).
68. Kuiper, L. M. et al. Epigenetic and Metabolomic Biomarkers for Biological Age: A Comparative Analysis of Mortality and Frailty Risk. J Gerontol A Biol Sci Med Sci 78, 1753 (2023).
69. Bogaards, F. A. et al. Secondary integrated analysis of multi-tissue transcriptomic responses to a combined lifestyle intervention in older adults from the GOTO nonrandomized trial. Nature Communications 2024 15:1 15, 1–18 (2024).
70. Plaza-Diaz, J. et al. Impact of Physical Activity and Exercise on the Epigenome in Skeletal Muscle and Effects on Systemic Metabolism. Biomedicines 10, (2022).
71. Pujar, M. K., Vastrad, B. & Vastrad, C. Integrative analyses of genes associated with subcutaneous insulin resistance. Biomolecules 9, (2019).
72. Mokbel, N. et al. Grb10 Deletion Enhances Muscle Cell Proliferation, Differentiation and GLUT4 Plasma Membrane Translocation. J Cell Physiol 229, 1753–1764 (2014).

73. Holt, L. J. et al. Grb10 regulates the development of fiber number in skeletal muscle. The FASEB Journal 26, 3658–3669 (2012).
74. Johnson, M. L. et al. Mechanism by which caloric restriction improves insulin sensitivity in sedentary obese adults. Diabetes 65, 74–84 (2016).
5. Dubé, J. J. et al. Effects of weight loss and exercise on insulin resistance, and intramyocellular triacylglycerol, diacylglycerol and ceramide. Diabetologia 54, 1147–1156 (2011).
76. Roberts, C. K., Hevener, A. L. & Barnard, R. J. Metabolic syndrome and insulin resistance: Underlying causes and modification by exercise training. Compr Physiol 3, 1–58 (2013).
77. Haizlip, K. M., Harrison, B. C. & Leinwand, L. A. Sex-based differences in skeletal muscle kinetics and fiber-type composition. Physiology 30, 30–39 (2015).
78. Deelen, J. et al. A metabolic profile of all-cause mortality risk identified in an observational study of 44,168 individuals. Nat Commun 10, (2019).
79. Leenders, M. et al. Protein supplementation during resistance-type exercise training in the elderly. Med Sci Sports Exerc 45, 542–552 (2013).
80. Van Dongen, E. J. et al. Translation of a tailored nutrition and resistance exercise intervention for elderly people to a real-life setting: adaptation process and pilot study. BMC Geriatr 17, 1–15 (2017).
81. Sinke, L., Cats, D. & Heijmans, B. T. Omixer: multivariate and reproducible sample randomization to proactively counter batch effects in omics studies. Bioinformatics 37, 3051–3052 (2021).
82. Sinke, L., van Iterson, M., Cats, D., Kuipers, T. & Heijmans, B. DNAmArray: Streamlined workflow for the quality control, normalization, and analysis of Illumina methylation array data. doi:10.5281/ZENODO.16962439.
83. Van Iterson, M. et al. MethylAid: visual and interactive quality control of large Illumina 450k datasets. Bioinformatics 30, 3435–3437 (2014).
84. Van Iterson, M., Cats, D., Hop, P. & Heijmans, B. T. omicsPrint: detection of data linkage errors in multiple omics studies. Bioinformatics 34, 2142–2143 (2018).
85. Zhou, W., Laird, P. W. & Shen, H. Comprehensive characterization, annotation and innovative use of Infinium DNA methylation BeadChip probes. Nucleic Acids Res 45, e22 (2017).
86. Sugden, K. et al. Patterns of Reliability: Assessing the Reproducibility and Integrity of DNA Methylation Measurement. Patterns 1, (2020).
87. Amemiya, H. M., Kundaje, A. & Boyle, A. P. The ENCODE Blacklist: Identification of Problematic Regions of the Genome. Scientific Reports 2019 9:1 9, 1–5 (2019).
88. Zhernakova, D. V. et al. Identification of context-dependent expression quantitative trait loci in whole blood. Nat Genet 49, 139–145 (2017).
89. Xie, X. et al. Single-cell transcriptomic landscape of human blood cells. Natl Sci Rev 8, (2021).
90. Koestler, D. C. et al. Improving cell mixture deconvolution by identifying optimal DNA methylation libraries (IDOL). BMC Bioinformatics 17, (2016).
91. Salas, L. A. et al. Enhanced cell deconvolution of peripheral blood using DNA methylation for high-resolution immune profiling. Nature Communications 2022 13:1 13, 1–13 (2022).
92. van Iterson, M. et al. Controlling bias and inflation in epigenome- and transcriptome-wide association studies using the empirical null distribution. Genome Biol 18, 1–13 (2017).
93. Slieker, R. C. et al. Identification and systematic annotation of tissue-specific differentially methylated regions using the Illumina 450k array. Epigenetics Chromatin 6, (2013).
94. Heinz, S. et al. Simple combinations of lineage-determining transcription factors prime cis-regulatory elements required for macrophage and B cell identities. Mol Cell 38, 576–589 (2010).
95. Lawrence, M. et al. Software for Computing and Annotating Genomic Ranges. PLoS Comput Biol 9, (2013).
96. Bonder, M. J. et al. Disease variants alter transcription factor levels and methylation of their binding sites. Nat Genet 49, 131–138 (2017).
97. Wang, Y., Grant, O. A., Zhai, X., Mcdonald-Maier, K. D. & Schalkwyk, L. C. Insights into ageing rates comparison across tissues from recalibrating cerebellum DNA methylation clock. Geroscience 46, 39–56 (2024).

Supplementary Material

Supplementary Figure 1 | Cross-tissue effect sizes. a. CpGs with significant responses in muscle, ordered by effect size in muscle and shown for all tissues (row 1: muscle, row 2: adipose, row 3: blood). **b.** CpGs with significant responses in adipose, ordered by effect size in adipose and shown for all tissues. **c.** CpGs with significant responses in blood, ordered by effect size in blood and shown for all tissues. Bars are coloured by FDR-adjusted *p*-value.

	Entire GOTO population (n = 164)		Three tissue overlap (n = 66)		Skeletal muscle (n = 80)		Adipose tissue (n = 89)		Fasted blood (n = 98)	
	Mean	SD	Mean	SD	Mean	SD	Mean	SD	Mean	SD
Body mass index (kg/m^2)	26.9	2.5	26.9	2.4	26.8	2.3	26.9	2.4	26.8	2.4
WC (cm)	96.1	8.0	97.0	7.3	96.9	7.4	96.1	7.4	96.1	7.5
Total body fat (%)	32.6	8.2	32.2	7.7	31.1	7.8	33.4	7.7	32.5	8.0
Fasting insulin (mU/L)	9.2	4.6	9.4	4.4	9.0	4.2	9.1	4.4	9.0	4.4
Systolic BP (mm Hg)	139.9	17.1	140.4	15.7	139.7	15.7	138.3	15.7	138.1	15.6
Leptin (µg/L)	14.0	10.6	13.0	9.0	11.9	8.6	14.9	10.6	14.1	10.4
Adiponectin (mg/L)	10.4	5.3	9.8	4.5	9.8	4.7	10.6	4.8	10.7	4.9
Interleukin-6 (ng/L)	1.4	1.8	1.1	0.7	1.2	1.3	1.0	0.7	1.2	1.2
HDL cholesterol (mmol/L)	9.6	0.2	9.6	0.2	9.5	0.2	9.6	0.2	9.6	0.2
Fasting HDL size (nm)	1.5	0.4	1.5	0.4	1.4	0.4	1.5	0.4	1.5	0.4

Supplementary Table 1 | Baseline characteristics in the GOTO population and tissue subsets.

	Three tissue overlap (n = 66)		Skeletal muscle (n = 80)		Adipose tissue (n = 89)		Fasted blood (n = 98)	
	Δ (SE)	p_{FDR}	Δ (SE)	p_{FDR}	Δ (SE)	p_{FDR}	Δ (SE)	p_{FDR}
Body mass index (kg/m^2)	-0.18 (0.13)	3.1E-01	-0.28 (0.12)	1.3E-01	-0.30 (0.13)	1.7E-01	-0.36 (0.13)	6.1E-02
WC (cm)	-0.83 (0.85)	4.1E-01	-1.46 (0.83)	2.6E-01	-0.39 (0.83)	8.0E-01	-0.74 (0.84)	5.4E-01
Total body fat (%)	-0.62 (0.47)	3.1E-01	-0.50 (0.46)	4.3E-01	-0.90 (0.47)	2.3E-01	-0.70 (0.47)	2.8E-01
Fasting insulin (mU/L)	-0.83 (0.52)	3.1E-01	-0.43 (0.50)	4.9E-01	-0.27 (0.49)	8.0E-01	-0.35 (0.50)	5.4E-01
Systolic BP (mm Hg)	0.48 (2.00)	8.1E-01	0.88 (1.89)	6.4E-01	0.56 (1.87)	8.5E-01	1.57 (1.88)	5.4E-01
Leptin (µg/L)	-0.65 (0.65)	4.1E-01	-0.70 (0.67)	4.3E-01	-1.27 (0.69)	2.3E-01	-1.23 (0.74)	2.4E-01
Adiponectin (mg/L)	0.45 (0.30)	3.1E-01	0.38 (0.29)	4.3E-01	0.05 (0.28)	8.6E-01	0.07 (0.29)	8.1E-01
Interleukin-6 (ng/L)	0.35 (0.22)	3.1E-01	0.27 (0.22)	4.3E-01	0.33 (0.23)	3.3E-01	0.42 (0.24)	2.4E-01
HDL cholesterol (mmol/L)	0.02 (0.03)	7.3E-01	0.02 (0.03)	6.4E-01	-0.02 (0.03)	8.0E-01	-0.02 (0.03)	5.4E-01
Fasting HDL size (nm)	0.02 (0.01)	3.1E-01	0.05 (0.01)	1.4E-03	0.02 (0.01)	3.3E-01	0.03 (0.01)	7.2E-02

Supplementary Table 2 | Non-response analysis comparing changes in health parameters in included and excluded individuals.

Nuclei type	Baseline	SD	beta	SE	p	p_{FDR}
Endothelial	36.57 %	7.06	3.26	0.90	5.03E-04	3.52E-03
Fibro-adipogenic progenitor	0.02 %	0.11	0.13	0.05	1.65E-02	5.76E-02
Satellite	<0.001 %	<0.001	0.08	0.04	3.74E-02	8.74E-02
Slow (type I) fibre	35.96 %	17.32	-2.01	2.35	3.95E-01	6.91E-01
Fast (type II) fibre	26.75 %	19.90	-1.51	2.36	5.24E-01	7.33E-01
Immune	0.69 %	1.56	0.05	0.22	8.34E-01	8.34E-01
Smooth muscle	0.01 %	0.11	0.004	0.02	8.10E-01	8.34E-01

Supplementary Table 3 | Baseline percentages and changes in predicted muscle nuclei types.

CpG	Position	beta	SE	p	p_{FDR}	n
cg12394201	chr11: 43942417	-0.0624	0.0085	1.40E-11	1.06E-05	147
cg24161080	chr18: 33889786	-0.0839	0.0117	3.56E-11	1.35E-05	148
cg05008948	chr7: 99160713	-0.0308	0.0046	7.40E-10	1.86E-04	148
cg01668986	chr8: 21541541	-0.0435	0.0068	2.86E-09	4.92E-04	148
cg21342383	chr10: 127661991	-0.0187	0.0029	3.26E-09	4.92E-04	148
cg13585930	chr10: 72027356	-0.0564	0.0089	5.23E-09	6.59E-04	148
cg07626206	chr7: 55200656	-0.0287	0.0046	6.37E-09	6.88E-04	147
cg02632441	chr2: 218711231	-0.0249	0.0040	1.06E-08	9.97E-04	148
cg25834201	chr1: 59949992	-0.0294	0.0049	2.30E-08	1.93E-03	148
cg12772738	chr20: 36616990	-0.0451	0.0075	2.76E-08	2.08E-03	148
cg25981106	chr1: 209824796	-0.0362	0.0061	3.75E-08	2.58E-03	148
cg07327489	chr9: 134554052	-0.0183	0.0031	4.33E-08	2.73E-03	148
cg02331902	chr5: 90610302	-0.0132	0.0023	7.14E-08	4.15E-03	148
cg22898055	chr7: 75581160	-0.0511	0.0088	8.59E-08	4.37E-03	148
cg04451259	chr11: 35358923	-0.0594	0.0102	8.68E-08	4.37E-03	148
cg25225070	chr11: 9587742	-0.0286	0.0050	1.08E-07	4.84E-03	148
cg18648613	chr4: 102153422	-0.0241	0.0042	1.09E-07	4.84E-03	148
cg01266377	chr8: 128920442	-0.0291	0.0051	1.20E-07	5.06E-03	148
cg16477554	chr3: 24198188	-0.0425	0.0074	1.29E-07	5.12E-03	148
cg03128029	chr2: 203143287	-0.0312	0.0055	1.45E-07	5.49E-03	148

Supplementary Table 4 | Top 20 CpGs differentially methylated in muscle after the intervention accounting for changes in predicted endothelial nuclei proportions.

	Male skeletal muscle reference epigenome (E107)			Female skeletal muscle reference epigenome (E108)		
Chromatin state	**OR**	p	p_{FDR}	**OR**	p	p_{FDR}
Active TSS	0.0893	6.75E-04	3.37E-03	0.1171	2.24E-03	1.12E-02
Flanking active TSS	1.3482	2.02E-01	3.78E-01	1.6381	4.78E-02	1.02E-01
Flanking transcribed	1.7736	5.68E-01	8.52E-01	2.3216	4.02E-01	6.29E-01
Transcribed region	0.4532	8.11E-02	1.74E-01	0.2334	3.81E-02	1.02E-01
Weakly transcribed	1.1973	4.24E-01	7.06E-01	1.2288	4.19E-01	6.29E-01
Genic enhancer	4.3410	2.61E-06	1.96E-05	3.5642	1.09E-03	8.20E-03
Enhancer	7.1539	4.53E-35	6.79E-34	5.8304	2.50E-21	3.75E-20
Znf/Rpts	0.0001	9.38E-01	9.38E-01	0.0001	9.46E-01	9.46E-01
Heterochromatin	0.0001	8.95E-01	9.38E-01	0.0001	9.08E-01	9.46E-01
Bivalent TSS	0.0001	8.22E-01	9.38E-01	0.0001	8.44E-01	9.46E-01
Flanking bivalent	0.0001	8.14E-01	9.38E-01	0.0001	7.61E-01	9.46E-01
Bivalent enhancer	0.0001	8.20E-01	9.38E-01	0.0001	8.42E-01	9.46E-01
Polycomb repressed	0.1976	2.25E-02	5.64E-02	0.2593	5.44E-02	1.02E-01
Weak polycomb repressed	0.3959	1.00E-02	3.01E-02	0.4559	4.27E-02	1.02E-01
Quiescent	0.4737	1.40E-03	5.26E-03	0.6117	4.41E-02	1.02E-01

Supplementary Table 5 | Chromatin state enrichment analysis for muscle CpGs using the male (E107) and female (E108) skeletal muscle reference epigenomes from the Roadmap Epigenomics Consortium.

Motif Name	Consensus	p	Target n (%)	Background (%)
AP-1	VTGACTCATC	1.44E-25	36 (22.22)	2.18
Atf3	DATGASTCATHN	3.34E-25	34 (20.99)	1.91
Bach1	AWWNTGCTGAGTCAT	1.13E-04	4 (2.47)	0.15
Bach2	TGCTGAGTCA	1.27E-12	14 (8.64)	0.58
BATF	DATGASTCAT	1.33E-26	35 (21.60)	1.87
Fos	NDATGASTCAYN	9.07E-29	35 (21.60)	1.61
Fosl2	NATGASTCABNN	4.08E-26	28 (17.28)	0.99
Fra1	NNATGASTCATH	4.22E-27	33 (20.37)	1.52
Fra2	GGATGACTCATC	5.28E-25	30 (18.52)	1.35
HIF-1a	TACGTGCV	4.26E-03	7 (4.32)	1.24
Jun-AP1	GATGASTCATCN	6.20E-21	22 (13.58)	0.76
JunB	RATGASTCAT	1.97E-27	34 (20.99)	1.62
MafA	TGCTGACTCA	6.75E-05	13 (8.02)	2.19
MafB	WNTGCTGASTCAGCANWTTY	7.25E-04	7 (4.32)	0.90
MafK	GCTGASTCAGCA	4.36E-04	6 (3.70)	0.59
NF-E2	GATGACTCAGCA	2.43E-07	6 (3.70)	0.16
NFkB-p65-Rel	GGAAATTCCC	2.51E-04	3 (1.85)	0.07
Nrf2	HTGCTGAGTCAT	9.78E-08	6 (3.70)	0.13
RUNX1	AAACCACARM	1.74E-05	14 (8.64)	2.22
RUNX-AML	GCTGTGGTTW	6.67E-04	9 (5.56)	1.45

Supplementary Table 6 | TFBS enrichment analysis in sequences within 50bp of muscle CpGs. The percentage of background sequences within 50bp of the respective motif is also shown.

CpG	Gene	Ensembl ID	log_2FC	p_{FDR}	eQTM	SE	p_{FDR}
cg17411016	*MCFD2*	ENSG00000180398	-0.1464	7.59E-06	0.1574	0.0172	6.50E-13
cg09312464	*FSCN1*	ENSG00000075618	0.3990	1.41E-05	-0.0325	0.0043	3.54E-10
cg13585930	*LRRC20*	ENSG00000172731	-0.2115	2.16E-06	0.1950	0.0257	3.54E-10
cg12595459	*EXTL3*	ENSG00000012232	-0.1339	8.65E-04	0.0883	0.0121	1.22E-09
cg21730012	*INPP5A*	ENSG00000068383	-0.2053	3.58E-06	0.0813	0.0128	1.01E-07
cg02849956	*DPP9*	ENSG00000142002	-0.1718	7.13E-06	0.1341	0.0208	1.01E-07
cg20748397	*FLII*	ENSG00000177731	-0.2214	2.86E-06	0.0837	0.0135	1.63E-07
cg03045139	*LHFPL2*	ENSG00000145685	0.3691	4.54E-06	-0.0294	0.0048	1.72E-07
cg02233071	*RUNX1*	ENSG00000159216	0.7576	4.54E-06	-0.0196	0.0035	2.46E-06
cg20748397	*ALKBH5*	ENSG00000091542	-0.1247	9.39E-04	0.0934	0.0169	2.86E-06
cg25981106	*HSD11B1*	ENSG00000117594	-0.4646	3.79E-07	0.0364	0.0066	3.51E-06
cg17411016	*TTC7A*	ENSG00000068724	0.2008	2.61E-03	-0.0476	0.0086	3.51E-06
cg21005024	*GRB10*	ENSG00000106070	-0.2544	2.13E-04	0.0831	0.0157	7.08E-06
cg14426392	*ATP1A1*	ENSG00000163399	0.2351	5.87E-05	-0.0735	0.0150	3.44E-05
cg17357895	*EXOC3L1*	ENSG00000179044	0.2516	2.58E-04	-0.0554	0.0114	3.44E-05
cg12402318	*TMOD3*	ENSG00000138594	0.2408	7.59E-06	-0.0346	0.0071	3.52E-05
cg20748397	*GID4*	ENSG00000141034	-0.1100	6.51E-03	0.0759	0.0159	4.59E-05
cg07827395	*FAM220A*	ENSG00000178397	-0.2584	5.87E-05	0.0502	0.0106	5.09E-05
cg07827395	*RAC1*	ENSG00000136238	-0.1316	1.83E-04	0.0875	0.0190	8.74E-05
cg20617626	*ARHGEF17*	ENSG00000110237	0.1426	5.99E-04	-0.0406	0.0089	9.56E-05

Supplementary Table 7 | Top 20 differentially expressed genes in muscle that were also associated with DNAm changes at nearby CpGs. The CpG and genes are shown alongside the log_2FC and its significance (FDR-adjusted *p*-value), as well as the eQTM correlation, SE, and adjusted p-value.

CpG	Trait	Effect size	SE	*p*	p_{FDR}
cg27187848	Waist circumference	0.0023	0.0005	1.15E0-5	1.15E-04
cg16350675	Leptin levels	-0.0025	0.0006	4.12E-05	4.12E-04
cg17411016	Waist circumference	0.0022	0.0006	1.25E-04	1.25E-03
cg25114611	Leptin levels	-0.0021	0.0005	1.98E-04	1.98E-03
cg13733654	Waist circumference	-0.0007	0.0002	2.90E-04	2.90E-03
cg11835462	Leptin levels	-0.0023	0.0006	3.30E-04	3.30E-03
cg25114611	Waist circumference	-0.0015	0.0004	8.41E-04	4.21E-03
cg27187848	HDL cholesterol size	-0.0987	0.0290	8.99E-04	4.49E-03
cg13306815	Leptin levels	-0.0028	0.0008	5.67E-04	5.67E-03
cg12386285	Leptin levels	-0.0009	0.0002	5.72E-04	5.72E-03
cg12772738	Leptin levels	-0.0037	0.0011	7.35E-04	7.35E-03
cg17411016	Body fat percentage	0.0035	0.0011	2.00E-03	8.01E-03
cg17411016	HDL cholesterol size	-0.1015	0.0327	2.40E-03	8.01E-03
cg14435903	Adiponectin levels	-0.0028	0.0008	1.01E-03	1.01E-02
cg18710458	Body fat percentage	0.0046	0.0014	1.03E-03	1.03E-02
cg02501746	Leptin levels	-0.0023	0.0007	1.04E-03	1.04E-02
cg25628315	Leptin levels	-0.0026	0.0008	1.10E-03	1.10E-02
cg25225070	HDL cholesterol size	-0.1073	0.0326	1.34E-03	1.21E-02
cg25225070	Adiponectin levels	-0.0035	0.0011	2.41E-03	1.21E-02
cg19768360	HDL cholesterol size	0.0860	0.0263	1.41E-03	1.41E-02

Supplementary Table 8 | Top 20 associations between muscle CpGs and immunometabolic health markers.

CpG	Trait	beta	SE	p	p_{FDR}
cg09312464	PAX7+ cells per fibre	-0.1575	0.0239	1.62E-09	4.85E-09
cg15982707	PAX7+ cells per fibre	-0.2593	0.0397	2.44E-09	7.33E-09
cg24161080	PAX7+ cells per fibre	-0.4751	0.0743	4.34E-09	1.30E-08
cg17633300	PAX7+ cells per fibre	-0.1146	0.0182	7.11E-09	2.13E-08
cg11012616	PAX7+ cells per fibre	-0.2104	0.0333	9.42E-09	2.83E-08
cg17411016	PAX7+ cells per fibre	-0.1907	0.0304	1.00E-08	3.01E-08
cg25981106	PAX7+ cells per fibre	-0.2723	0.0438	1.19E-08	3.56E-08
cg01668986	PAX7+ cells per fibre	-0.3013	0.0493	1.82E-08	5.45E-08
cg17370665	PAX7+ cells per fibre	-0.2303	0.0379	2.38E-08	7.15E-08
cg17357895	PAX7+ cells per fibre	-0.3072	0.0513	2.89E-08	8.68E-08
cg21730012	PAX7+ cells per fibre	-0.1683	0.0283	3.74E-08	1.12E-07
cg00545756	PAX7+ cells per fibre	-0.2086	0.0354	4.51E-08	1.35E-07
cg27461254	PAX7+ cells per fibre	-0.1996	0.0340	5.53E-08	1.66E-07
cg14343713	PAX7+ cells per fibre	-0.1446	0.0246	6.67E-08	2.00E-07
cg25132536	PAX7+ cells per fibre	-0.3268	0.0562	7.41E-08	2.22E-07
cg12166519	PAX7+ cells per fibre	-0.1852	0.0321	8.66E-08	2.60E-07
cg27187848	PAX7+ cells per fibre	-0.1576	0.0276	1.22E-07	3.66E-07
cg20617626	PAX7+ cells per fibre	-0.1231	0.0217	1.30E-07	3.90E-07
cg04814966	myonuclei per fibre	-0.0075	0.0014	3.29E-07	5.15E-07
cg04814966	PAX7+ cells per fibre	-0.1258	0.0231	3.43E-07	5.15E-07

Supplementary Table 9 | Top 20 associations between DNAm at muscle CpGs and immunohistochemistry markers.

Cell type	Baseline	SD	Delta	SE	p	p_{FDR}
Adipocytes	72.45 %	7.83	-0.40	0.99	6.87E-01	7.28E-01
CD4+ T-cells	0.15 %	0.50	-0.08	0.06	2.00E-01	7.28E-01
MVECs	24.06 %	6.53	0.32	0.92	7.28E-01	7.28E-01
M1 Macrophages	0.03 %	0.16	0.03	0.04	3.73E-01	7.28E-01
M2 Macrophages	3.31 %	2.26	0.12	0.19	5.20E-01	7.28E-01

Supplementary Table 10 | Baseline percentages and changes in predicted adipose tissue cell types.

CpG	Position	beta	SE	p	p_{FDR}	n
cg12544951	chr20: 21695342	0.0738	0.0119	3.66E-09	1.24E-03	178
cg06524692	chr1: 28864470	0.0257	0.0041	4.03E-09	1.24E-03	178
cg01733176	chr4: 111561069	-0.0396	0.0064	5.50E-09	1.24E-03	178
cg03475429	chr10: 94982392	0.0236	0.0039	6.58E-09	1.24E-03	178
cg08156066	chr20: 21695333	0.0636	0.0105	9.56E-09	1.44E-03	178
cg05844247	chr20: 21694427	0.0632	0.0106	1.72E-08	1.64E-03	178
cg07931189	chr2: 53463157	-0.0338	0.0057	1.77E-08	1.64E-03	178
cg10629004	chr20: 21696466	0.0447	0.0075	1.90E-08	1.64E-03	178
cg13655674	chr1: 119522385	-0.0210	0.0035	1.97E-08	1.64E-03	178
cg07213060	chr20: 21694826	0.0681	0.0115	2.17E-08	1.64E-03	178
cg18574731	chr10: 116415067	0.0192	0.0033	3.04E-08	2.09E-03	178
cg17596409	chr4: 153186304	0.0652	0.0112	3.67E-08	2.31E-03	178
cg15556943	chr20: 21694616	0.0765	0.0133	4.50E-08	2.51E-03	178
cg06032603	chr9: 38127746	0.0411	0.0071	4.65E-08	2.51E-03	178
cg22888671	chr17: 26799382	0.0215	0.0037	5.13E-08	2.58E-03	178
cg17908503	chr20: 21690788	0.0566	0.0099	6.55E-08	2.91E-03	178
cg19404433	chr20: 21695772	0.0333	0.0058	6.55E-08	2.91E-03	177
cg18059621	chr2: 105486198	0.0303	0.0053	7.46E-08	3.13E-03	178
cg00497086	chr16: 23869599	0.0215	0.0038	9.94E-08	3.76E-03	178
cg20432507	chr20: 21689860	0.0493	0.0088	9.96E-08	3.76E-03	178

Supplementary Table 11 | Top 20 CpGs differentially methylated after the intervention in adipose tissue.

Chromatin state	OR	p	p_{FDR}
Active TSS	0.1051	1.04E-04	5.21E-04
Flanking active TSS	0.1271	3.45E-05	2.59E-04
Flanking transcribed	0.0001	9.22E-01	9.87E-01
Transcribed region	0.3265	3.51E-03	1.05E-02
Weakly transcribed	0.5178	1.35E-02	2.90E-02
Genic enhancer	0.0001	7.91E-01	9.87E-01
Enhancer	0.3798	4.41E-03	1.10E-02
Znf/Rpts	0.0001	9.18E-01	9.87E-01
Heterochromatin	0.9895	9.88E-01	9.88E-01
Bivalent TSS	0.0001	8.71E-01	9.87E-01
Flanking bivalent	1.1540	7.09E-01	9.87E-01
Bivalent enhancer	1.8753	8.07E-02	1.34E-01
Polycomb repressed	7.7623	4.90E-44	7.35E-43
Weak polycomb repr.	1.5008	2.09E-02	3.92E-02
Quiescent	1.6535	4.06E-04	1.52E-03

Supplementary Table 12 | Chromatin state enrichment analysis for identified CpGs using the adipocyte reference epigenome from the Roadmap Epigenomics Consortium (E063). The chromatin state, odds ratio (OR), and significance of the enrichment is shown (nominal and FDR-adjusted *p*-values; TSS: transcription start site).

Motif Name	Consensus	*p*	Target *n* (%)	Background (%)
Gata2(Zf)	BBCTTATCTS	3.73E-04	11 (4.78)	1.36
Gata6(Zf)	YCTTATCTBN	1.44E-03	12 (5.22)	1.86
Gata1(Zf)	SAGATAAGRV	2.58E-03	9 (3.91)	1.24
Fra2(bZIP)	GGATGACTCATC	6.62E-03	6 (2.61)	0.72
Tgif2(Homeobox)	TGTCANYT	6.75E-03	30 (13.04)	8.10
Gata4(Zf)	NBWGATAAGR	8.03E-03	11 (4.78)	2.03
Fra1(bZIP)	NNATGASTCATH	8.92E-03	6 (2.61)	0.76

Supplementary Table 13 | TFBS enrichment analysis in sequences within 50bp of identified CpGs in adipose tissue. The TF name and type is shown alongside its consensus motif, the significance of the enrichment, and the number and percentage of CpGs responsible for the enrichment. The percentage of background sequences within 50bp of the respective motif is also shown.

CpG	Gene	Ensembl ID	$\log_2$FC	p_{FDR}	eQTM	SE	p_{FDR}
cg02649849	*DMRT3*	ENSG00000064218	-0.3375	1.63E-03	0.0199	0.0018	8.13E-18
cg03148184	*PITX2*	ENSG00000164093	-0.2134	1.23E-02	0.0592	0.0058	1.21E-16
cg26708319	*PITX2*	ENSG00000164093	-0.2134	1.23E-02	0.0564	0.0057	5.18E-16
cg19370653	*PITX2*	ENSG00000164093	-0.2134	1.23E-02	0.0621	0.0065	1.68E-15
cg07790170	*PITX2*	ENSG00000164093	-0.2134	1.23E-02	0.0696	0.0074	8.49E-15
cg03943773	*PITX2*	ENSG00000164093	-0.2134	1.23E-02	0.0507	0.0056	1.89E-14
cg23646776	*PITX2*	ENSG00000164093	-0.2134	1.23E-02	0.0365	0.0040	3.67E-14
cg24005685	*PITX2*	ENSG00000164093	-0.2134	1.23E-02	0.0582	0.0065	4.44E-14
cg10895452	*EN1*	ENSG00000163064	-0.1853	4.64E-03	-0.0146	0.0017	1.64E-13
cg24925400	*PITX2*	ENSG00000164093	-0.2134	1.23E-02	0.0502	0.0059	6.84E-13
cg01951086	*PITX2*	ENSG00000164093	-0.2134	1.23E-02	0.0654	0.0079	2.24E-12
cg23806894	*PITX2*	ENSG00000164093	-0.2134	1.23E-02	0.0485	0.0063	2.44E-11
cg17242937	*PITX2*	ENSG00000164093	-0.2134	1.23E-02	0.0510	0.0067	4.32E-11
cg21299542	*PITX2*	ENSG00000164093	-0.2134	1.23E-02	0.0309	0.0041	4.71E-11
cg01733176	*PITX2*	ENSG00000164093	-0.2134	1.23E-02	0.0428	0.0060	4.01E-10
cg26023087	*DMRT3*	ENSG00000064218	-0.3375	1.63E-03	0.0157	0.0022	5.90E-10
cg19849728	*PITX2*	ENSG00000164093	-0.2134	1.23E-02	0.0380	0.0059	1.23E-08
cg14434922	*DMRT3*	ENSG00000064218	-0.3375	1.63E-03	0.0134	0.0022	8.69E-08
cg05581451	*PITX2*	ENSG00000164093	-0.2134	1.23E-02	0.0341	0.0058	2.06E-07
cg18792984	*TREM1*	ENSG00000124731	-0.3144	1.27E-02	0.0170	0.0029	2.33E-07

Supplementary Table 14 | Top 20 differentially expressed genes in adipose tissue that were also associated with DNAm changes at nearby CpGs. The CpG and associated gene identifiers are shown alongside the $\log_2$FC and its significance (FDR-adjusted *p*-value), and the eQTM effect size (eQTM), standard error (SE), and significance (FDR-adjusted p-value).

Database	Term	p_{FDR}	Overlapping genes
GO BP (2023)	Embryonic Organ Morphogenesis (GO:0048562)	1.27E-02	*ALX1, HOXB3, HOXB4*
GO BP (2023)	Phospholipid Efflux (GO:0033700)	1.86E-02	*APOC1, APOE*
GO BP (2023)	Regulation Of Transcription By RNA Polymerase II (GO:0006357)	1.86E-02	*ALX1, DMRT3, EN1, HOXB2, HOXB3, HOXB4, HOXB8, NR2F1, PITX2, SAP30L*
GO BP (2023)	High-Density Lipoprotein Particle Remodelling (GO:0034375)	1.86E-02	*APOC1, APOE*
Reactome (2022)	Plasma Lipoprotein Assembly R-HSA-8963898	1.86E-02	*APOC1, APOE*
Reactome (2022)	Activation Of HOX Genes During Differentiation R-HSA-5619507	1.86E-02	*HOXB2, HOXB3, HOXB4*
GO BP (2023)	Cholesterol Efflux (GO:0033344)	2.68E-02	*APOC1, APOE*
GO BP (2023)	Regulation Of DNA-templated Transcription (GO:0006355)	2.68E-02	*ALX1, APOE, DMRT3, EN1, HOXB3, HOXB4, HOXB8, PITX2, SAP30L*
GO BP (2023)	Hematopoietic Progenitor Cell Differentiation (GO:0002244)	3.32E-02	*ARMC6, HOXB4*
GO BP (2023)	Embryonic Skeletal System Morphogenesis (GO:0048704)	3.32E-02	*HOXB3, HOXB4*
GO BP (2023)	Positive Regulation Of DNA-templated Transcription (GO:0045893)	3.32E-02	*ALX1, APOE, HOXB2, HOXB3, HOXB4, NR2F1, PITX2*
GO BP (2023)	Embryonic Skeletal System Development (GO:0048706)	3.32E-02	*HOXB3, HOXB4*
Reactome (2022)	Plasma Lipoprotein Clearance R-HSA-8964043	3.32E-02	*APOC1, APOE*
Reactome (2022)	NR1H3 And NR1H2 Regulate Gene Expression Linked To Cholesterol Transport And Efflux	3.32E-02	*APOC1, APOE*
Reactome (2022)	Transcriptional Regulation By AP-2 (TFAP2) Family Of Transcription Factors	3.32E-02	*APOE, PITX2*
GO BP (2023)	Positive Regulation Of Transcription By RNA Polymerase II (GO:0045944)	3.32E-02	*ALX1, HOXB2, HOXB3, HOXB4, NR2F1, PITX2*
GO BP (2023)	Acylglycerol Metabolic Process (GO:0006639)	3.85E-02	*APOC1, APOE*
GO BP (2023)	Skeletal System Morphogenesis (GO:0048705)	4.00E-02	*HOXB3, HOXB4*
GO BP (2023)	Triglyceride Metabolic Process (GO:0006641)	4.12E-02	*APOC1, APOE*
Reactome (2022)	NR1H2 And NR1H3-mediated Signalling R-HSA-9024446	4.12×1-02	*APOC1, APOE*

Supplementary Table 15 | Top 20 enriched genes sets in differentially expressed genes in adipose tissue also associated with DNAm changes at nearby CpGs.

CpG	Trait	beta	SE	p	p_{FDR}
cg07219853	Interleukin-6 levels	-0.0211	0.0051	5.06E-05	5.06E-04
cg04715165	Interleukin-6 levels	-0.0211	0.0052	7.34E-05	7.34E-04
cg04543233	Body fat percentage	-0.0045	0.0011	8.96E-05	8.96E-04
cg06161697	Body fat percentage	0.0032	0.0008	9.22E-05	9.22E-04
cg03160217	Interleukin-6 levels	-0.0120	0.0030	1.02E-04	1.02E-03
cg20907471	Body fat percentage	-0.0062	0.0016	2.02E-04	2.02E-03
cg02355868	Fasting insulin levels	0.0026	0.0007	2.22E-04	2.22E-03
cg23994043	Interleukin-6 levels	0.0195	0.0052	2.29E-04	2.29E-03
cg02468230	Body fat percentage	0.0030	0.0008	2.81E-04	2.81E-03
cg04290158	Body fat percentage	0.0031	0.0009	3.15E-04	3.15E-03
cg23247845	Interleukin-6 levels	-0.0172	0.0047	3.33E-04	3.33E-03
cg02355868	Body fat percentage	0.0027	0.0008	7.26E-04	3.63E-03
cg12022722	Leptin levels	-0.0013	0.0003	3.69E-04	3.69E-03
cg17193941	Interleukin-6 levels	-0.0145	0.0040	4.21E-04	4.21E-03
cg10629004	Body fat percentage	-0.0055	0.0015	4.24E-04	4.24E-03
cg07213060	Interleukin-6 levels	0.0307	0.0086	4.50E-04	4.50E-03
cg23660235	Interleukin-6 levels	-0.0191	0.0054	4.76E-04	4.76E-03
cg07452809	Interleukin-6 levels	-0.0188	0.0053	5.04E-04	5.04E-03
cg02355868	Waist circumference	0.0012	0.0004	1.66E-03	5.55E-03
cg02621151	Interleukin-6 levels	0.0158	0.0045	5.60E-04	5.60E-03

Supplementary Table 16 | Top 20 associations between identified CpGs in adipose tissue and immunometabolic health markers. The CpG identifier and associated trait is shown alongside its effect size (beta), standard error (SE), and significances (nominal and FDR-adjusted *p*-value)

Measured cell type	Baseline	SD	Beta	SE	p	p_{FDR}
Neutrophils	50.37 %	8.50	0.215	0.666	7.48E-01	9.46E-01
Lymphocytes	36.89 %	8.36	-0.067	0.563	9.06E-01	9.46E-01
Monocytes	8.62 %	2.15	-0.034	0.209	8.73E-01	9.46E-01
Eosinophils	3.57 %	2.50	-0.128	0.145	3.78E-01	9.46E-01
Basophils	0.53 %	0.30	0.017	0.030	5.76E-01	9.46E-01
MuSiC cell types	**Baseline**	**SD**	**Beta**	**SE**	p	p_{FDR}
Mature neutrophils	28.89 %	5.35	0.812	0.607	1.84E-01	9.46E-01
Meta-myelocyte	24.48 %	4.92	0.065	0.637	9.18E-01	9.46E-01
Intermediate monocytes	20.87 %	5.37	-0.535	0.676	4.31E-01	9.46E-01
CD8+ T-cells	18.80 %	8.75	-1.604	0.948	9.45E-02	9.46E-01
Pre-monocyte	3.13 %	1.60	0.044	0.208	8.32E-01	9.46E-01
Classical monocytes	1.17 %	2.04	0.505	0.329	1.29E-01	9.46E-01
Immature B-cells	1.12 %	2.10	0.031	0.115	7.92E-01	9.46E-01
Non-classical monocytes	0.70 %	1.42	-0.201	0.230	3.84E-01	9.46E-01
CD4+ T-cells	0.29 %	2.00	1.012	0.679	1.38E-01	9.46E-01
Erythrocytes	0.20 %	0.27	-0.094	0.027	7.51E-04	2.07E-02
Naïve B-cells	0.11 %	1.02	-0.015	0.066	8.16E-01	9.46E-01
Common monocyte progenitors	0.09 %	0.46	-0.003	0.043	9.46E-01	9.46E-01
Myelocyte	0.08 %	0.71	-0.050	0.085	5.63E-01	9.46E-01
Plasma cells	0.03 %	0.06	-0.001	0.008	9.20E-01	9.46E-01
Monocyte-dendritic progenitors	0.02 %	0.10	0.012	0.023	6.09E-01	9.46E-01
Cytotoxic natural killer cells	0.01 %	0.03	0.001	0.003	6.46E-01	9.46E-01
Regulatory B-cells	<0.001 %	0.01	-0.001	0.001	4.22E-01	9.46E-01
IDOL cell types	**Baseline**	**SD**	**Beta**	**SE**	p	p_{FDR}
Neutrophils	51.84 %	7.66	-0.117	0.673	8.62E-01	9.46E-01
CD4+ T-cells	15.74 %	5.72	0.073	0.338	8.31E-01	9.46E-01
CD8+ T-cells	12.98 %	3.94	0.037	0.210	8.59E-01	9.46E-01
Monocytes	10.13 %	2.37	0.057	0.193	7.69E-01	9.46E-01
B-cells	6.52 %	4.57	0.130	0.128	3.12E-01	9.46E-01
Natural killer cells	5.88 %	3.09	-0.202	0.175	2.52E-01	9.46E-01
IDOLext cell types	**Baseline**	**SD**	**Beta**	**SE**	p	p_{FDR}
Neutrophils	47.72 %	8.78	-0.190	0.748	8.00E-01	9.46E-01
CD4+ memory T-cells	10.42 %	3.70	0.313	0.269	2.48E-01	9.46E-01
Monocytes	7.35 %	2.01	0.023	0.165	8.92E-01	9.46E-01
CD8+ memory T-cells	7.27 %	4.78	-0.102	0.215	6.35E-01	9.46E-01
CD4+ naïve T-cells	6.81 %	4.43	-0.122	0.185	5.12E-01	9.46E-01
Natural killer cells	5.59 %	2.43	-0.142	0.155	3.60E-01	9.46E-01
Naïve B-cells	3.60 %	1.73	0.096	0.081	2.41E-01	9.46E-01
Memory B-cells	2.38 %	4.91	-0.011	0.085	8.94E-01	9.46E-01
Eosinophils	2.37 %	2.45	-0.052	0.198	7.93E-01	9.46E-01
Regulatory T-cells	1.27 %	0.98	0.027	0.074	7.17E-01	9.46E-01
CD8+ naïve T-cells	0.76 %	1.27	0.083	0.071	2.43E-01	9.46E-01
Basophils	0.68 %	0.63	0.099	0.055	7.42E-02	9.46E-01

Supplementary Table 17 | Baseline percentages and changes in blood cell types using measured cell types and three deconvolution algorithms.

CpG	Position	beta	SE	p	p_{FDR}	n
cg23961638	chr4:153700210	-0.0029	0.0006	2.06E-09	9.50E-04	194
cg16209776	chr12:63177893	-0.0117	0.0023	2.51E-09	9.50E-04	196
cg26201957	chr11:82601012	-0.0278	0.0056	5.98E-09	1.23E-03	195
cg13479371	chr18:72530930	-0.0050	0.0010	6.72E-09	1.23E-03	196
cg25040733	chr5:141704733	0.0121	0.0024	8.12E-09	1.23E-03	194
cg08769073	chr11:12214803	0.0086	0.0018	1.32E-08	1.67E-03	196
cg17279445	chr4:188428636	0.0086	0.0018	2.42E-08	2.61E-03	193
cg09925408	chr19:1578728	0.0016	0.0003	4.72E-08	3.78E-03	196
cg06860177	chr10:122938108	-0.0182	0.0039	4.98E-08	3.78E-03	191
cg15280030	chr3:127637280	0.0097	0.0021	5.00E-08	3.78E-03	196
cg21196038	chr6:169560205	-0.0051	0.0011	6.60E-08	4.08E-03	194
cg07318969	chr9:101366405	0.0064	0.0014	6.96E-08	4.08E-03	196
cg09404334	chr6:86304179	-0.0049	0.0011	7.31E-08	4.08E-03	196
cg12484370	chr9:14314969	-0.0034	0.0007	7.62E-08	4.08E-03	192
cg17707984	chr6:31830405	-0.0033	0.0007	8.91E-08	4.08E-03	194
cg12559900	chr15:85268268	0.0023	0.0005	9.12E-08	4.08E-03	196
cg09910998	chr7:94285941	-0.0123	0.0027	9.17E-08	4.08E-03	196
cg13679891	chr1:177669461	0.0298	0.0065	9.72E-08	4.08E-03	194
cg16868350	chr19:55064372	0.0354	0.0077	1.13E-07	4.49E-03	190
cg00784718	chr1:221916685	-0.0069	0.0015	1.25E-07	4.74E-03	194

Supplementary Table 18 | Top 20 CpGs differentially methylated after the intervention in blood. The CpG identified and its position are shown alongside the intervention effect size (beta), its standard error (SE), significance (nominal and FDR-adjusted *p*-value), and sample size used to derive the effect (*n*).

Chromatin state	OR	p	p_{FDR}
Active TSS	1.2061	3.38E-01	7.23E-01
Flanking active TSS	1.4998	1.47E-03	1.11E-02
Flanking transcribed	1.1703	8.75E-01	9.67E-01
Transcribed region	1.2934	7.44E-02	3.72E-01
Weakly transcribed	0.9176	5.74E-01	9.43E-01
Genic enhancer	0.6663	4.84E-01	9.07E-01
Enhancer	0.6273	1.27E-01	4.75E-01
Znf/Rpts	1.3934	7.40E-01	9.43E-01
Heterochromatin	0.9704	9.59E-01	9.67E-01
Bivalent TSS	0.6468	3.33E-01	7.23E-01
Flanking bivalent	0.6379	3.17E-01	7.23E-01
Bivalent enhancer	1.1514	7.54E-01	9.43E-01
Polycomb repressed	0.3420	7.50E-04	1.11E-02
Weak polycomb repression	0.9326	6.37E-01	9.43E-01
Quiescent	0.9958	9.67E-01	9.67E-01

Supplementary Table 19 | Chromatin state enrichment analysis for identified CpGs using the PBMC reference epigenome from the Roadmap Epigenomics Consortium (E062). The chromatin state, odds ratio (OR), and significance of the enrichment is shown (nominal and FDR-adjusted *p*-values; TSS: transcription start site).

Motif Name	Consensus	*p*	Target *n* (%)	Background (%)
NFE2L2(bZIP)	AWWWTGCTGAGTCAT	1.00E-03	3 (0.68)	0.04%
Sox9(HMG)	AGGVNCCTTTGT	1.00E-02	13 (2.95)	1.23%
MafK(bZIP)	GCTGASTCAGCA	1.00E-02	6 (1.36)	0.36%

Supplementary Table 20 | TFBS enrichment analysis in sequences within 50bp of identified CpGs in blood. The TF name and type is shown alongside its consensus motif, the significance of the enrichment, and the number and percentage of CpGs responsible for the enrichment. The percentage of background sequences within 50bp of the respective motif is also shown.

CpG	Gene	Ensembl ID	$\log_2$FC	p_{FDR}	eQTM	SE	p_{FDR}
cg18032191	*LTBR*	ENSG00000111321	0.155	3.97E-03	-0.019	0.004	3.26E-05
cg18032191	*TNFRSF1A*	ENSG00000067182	0.123	1.65E-02	-0.018	0.004	7.55E-05
cg21095811	*ATG2B*	ENSG00000066739	-0.086	3.81E-02	-0.004	0.001	8.85E-03

Supplementary Table 21 | Differentially expressed genes in blood that were also associated with DNAm changes at nearby CpGs. The CpG and associated gene identifiers are shown alongside the $\log_2$FC and its significance (FDR-adjusted p-value), and the eQTM effect size (eQTM), SE and significance (FDR-adjusted *p*-value).

CpG	Trait	Beta	SE	*p*	p_{FDR}
cg16209776	Waist circumference	0.0011	0.0002	4.80E-06	4.80E-05
cg09222461	HDL cholesterol size	-0.0277	0.0061	1.62E-05	1.62E-04
cg16657397	Leptin levels	-0.0008	0.0002	2.73E-05	1.69E-04
cg16657397	Body fat percentage	-0.0014	0.0003	3.38E-05	1.69E-04
cg06612452	Waist circumference	0.0003	0.0001	4.58E-05	4.58E-04
cg07735194	Interleukin-6 levels	0.0086	0.0021	5.82E-05	5.82E-04
cg16610939	HDL cholesterol size	-0.0540	0.0131	6.46E-05	6.46E-04
cg17061897	Body mass index	0.0032	0.0008	7.04E-05	7.04E-04
cg08943940	HDL cholesterol size	-0.0423	0.0110	1.79E-04	1.79E-03
cg18945877	HDL cholesterol size	-0.0753	0.0197	1.91E-04	1.91E-03
cg17061897	Waist circumference	0.0007	0.0002	4.90E-04	2.45E-03
cg04103122	Leptin levels	0.0011	0.0003	3.52E-04	3.52E-03
cg27120531	Waist circumference	0.0011	0.0003	7.17E-04	3.79E-03
cg27120531	Body mass index	0.0043	0.0012	7.57E-04	3.79E-03
cg15815515	Body fat percentage	0.0060	0.0017	5.22E-04	5.22E-03
cg27422762	Body fat percentage	0.0036	0.0010	5.35E-04	5.35E-03
cg25440376	Systolic blood pressure	0.0002	0.0001	5.53E-04	5.53E-03
cg16209776	Leptin levels	0.0009	0.0003	1.42E-03	5.91E-03
cg16209776	Body fat percentage	0.0016	0.0005	1.77E-03	5.91E-03
cg24722351	Body fat percentage	0.0014	0.0004	6.31E-04	6.31E-03

Supplementary Table 22 | Top 20 associations between identified CpGs in blood and immunometabolic health markers. The CpG identifier and associated trait is shown alongside its effect size (beta), standard error (SE), and significances (nominal and FDR-adjusted *p*-value; HDL: high density lipoprotein)

cAge clock	Delta	Change in weeks	SE	p	p_{FDR}
Horvath (2013)	-0.430	-22.349	0.333	2.004E-01	2.004E-01
Zhang (2019)	-0.337	-17.503	0.116	4.542E-03	1.363E-02
Bernabeu cAge (2023)	-0.241	-12.545	0.147	1.031E-01	1.547E-01
Bernabeu bAge (2023)	-0.3092	-16.0803	0.2639	2.44E-01	2.44E-01
grimAge	-0.6658	-34.6191	0.1542	3.61E-05	1.44E-04
phenoAge	-0.7788	-40.4974	0.3751	4.04E-02	5.39E-02
MEAT	-1.1125	-57.8510	0.4230	1.03E-02	2.05E-02

Supplementary Table 23 | Predictions of change in biological (bAge) and chronological (cAge) age following the GOTO intervention using various algorithms. The estimated change (shown in years and weeks) is shown alongside the standard error (SE) and significance (nominal and FDR-adjusted *p*-values).

bAge clock	Trait	beta	SE	p	p_{FDR}
grimAge	Body mass index	0.2983	0.0844	5.21E-04	5.21E-03
grimAge	Waist circumference	0.0733	0.0199	3.25E-04	5.21E-03
grimAge	Leptin levels	0.0847	0.0268	1.89E-03	1.26E-02
grimAge	Body fat percentage	0.1013	0.0406	1.37E-02	3.91E-02
grimAge	Fasting insulin	0.1064	0.0411	1.07E-02	3.91E-02
grimAge	Interleukin-6 levels	0.3027	0.1179	1.13E-02	3.91E-02
grimAge	HDL cholesterol size	-3.2202	1.2836	1.30E-02	3.91E-02
grimAge	Adiponectin levels	-0.1249	0.0572	3.02E-02	7.56E-02
grimAge	HDL cholesterol levels	-0.9049	0.5631	1.10E-01	2.44E-01
MEAT	Leptin levels	0.0619	0.0535	2.50E-01	5.00E-01
MEAT	HDL cholesterol levels	1.1047	1.0718	3.05E-01	5.54E-01
MEAT	Interleukin-6 levels	0.1971	0.2185	3.69E-01	6.15E-01
grimAge	Systolic blood pressure	0.0063	0.0114	5.84E-01	7.67E-01
MEAT	Waist circumference	0.0181	0.0400	6.52E-01	7.67E-01
MEAT	Body fat percentage	0.0465	0.0798	5.61E-01	7.67E-01
MEAT	Fasting insulin	-0.0392	0.0786	6.19E-01	7.67E-01
MEAT	Systolic blood pressure	-0.0099	0.0217	6.47E-01	7.67E-01
MEAT	Body mass index	0.0439	0.1430	7.60E-01	8.44E-01
MEAT	Adiponectin levels	-0.0148	0.0897	8.69E-01	8.90E-01
MEAT	HDL cholesterol size	0.3155	2.2756	8.90E-01	8.90E-01

Supplementary Table 24 | Associations between bAge as measured by MEAT and grimAge, and ten health parameters. The algorithm used and associated trait is shown alongside the effect size (beta), its standard error (SE), and significance (nominal and FDR-adjusted *p*-value; HDL: high density lipoprotein)